AMERICAN UNIVERSITY OF BEIRUT

OPTIMAL CONFIGURATION AND ENERGY DISPATCH
STRATEGIES OF POWER SOURCES IN COMMUNITY
MICROGRID UNDER SCHEDULED BLACKOUTS

by
AHMAD DEEB SAWWAS

A thesis
submitted in partial fulfillment of the requirements
for the degree of Master of Engineering
to the Department of Electrical and Computer Engineering
of the Maroun Semaan Faculty of Engineering and Architecture
at the American University of Beirut

Beirut, Lebanon
February 2018

OPTIMAL CONFIGURATION AND ENERGY DISPATCH STRATEGIES OF POWER SOURCES IN COMMUNITY MICROGRID UNDER SCHEDULED BLACKOUTS

by

AHMAD DEEB SAWWAS

Approved by:

_____   _____
Dr. Riad Chedid, Professor   Advisor
Electrical and Computer Engineering

_____   _____
Dr. Sami Karaki   Member of Committee
Electrical and Computer Engineering

_____   _____
Dr. Ali Bazzi, Associate Professor   Member of Committee
Electrical and Computer Engineering

_____   _____
Dr. Raymond Ghajar, Professor   Member of Committee
School of Engineering /Electrical & Computer Engineering

Date of thesis/dissertation defense: February 18, 2020

AMERICAN UNIVERSITY OF BEIRUT

THESIS, DISSERTATION, PROJECT RELEASE FORM

Student Name: _Sawwas_ _Ahmad_ _Deeb_
                Last   First   Middle

(✓) Master's Thesis   ◯ Master's Project   ◯ Doctoral
Dissertation

[✓]   I authorize the American University of Beirut to: (a) reproduce hard or electronic copies of my thesis, dissertation, or project; (b) include such copies in the archives and digital repositories of the University; and (c) make freely available such copies to third parties for research or educational purposes.

[ ]   I authorize the American University of Beirut, to: (a) reproduce hard or electronic copies of it; (b) include such copies in the archives and digital repositories of the University; and (c) make freely available such copies to third parties for research or educational purposes

after : **One ----   year from the date of submission of my thesis, dissertation, or project.**
        Two ----   years from the date of submission of my thesis, dissertation, or project.
        Three ---- years from the date of submission of my thesis, dissertation, or project.

_____   _Friday 21, Feb , 2020_

Signature   Date

ACKNOWLEDGEMENT

AN ABSTRACT OF THE THESIS OF

Ahmad Deeb Sawwas   for   Master of Engineering
                                           Major: Energy and Power Systems

Title: Optimal Configuration and Energy Dispatch Strategies of Power Sources in Community Microgrid Under Scheduled Blackouts

In order to embrace the integration of distributed energy resources in distribution networks, microgrids are formed. However, despite the significant performance microgrid had revealed, it still fails in providing a reliable source of energy especially when operating in islanded mode. Therefore, in an attempt to improve reliability and utilize the large amount of microgrids implemented, the idea of combining microgrids located in closed proximities, thus forming a microgrids community, became more attractive.

The basic idea behind community microgrid is to connect multiple distributed energy resources, owned by several owners, in order to satisfy the community's energy demand in the most feasible and reliable manner. However, one of the major obstacles faced when forming a microgrid community is developing its market model. Each microgrid or distributed energy resource within a microgrid community is owned by a certain owner, thus implementing a microgrid community must be accompanied by developing a market model which governs the energy traded between its participants.

The following work illustrates a study made to test the potential of implementing community microgrid in distribution networks characterized by scheduled blackouts and heavy diesel reliance. Achieving such objective, two main steps are to be implemented. The first one aims to optimize each microgrid with an optimal energy resources configuration along with an optimal dispatch strategy that minimizes each microgrid's daily operational cost. The second step aims to test the applicability and attractiveness of connecting these microgrids together through forming a suitable pool-based day-ahead energy market.

Assessing the attractiveness of the proposed market is to be demonstrated through checking each microgrid's participation profile in the proposed market model, along with its new annual operational cost.

CONTENTS

ILLUSTRATIONS

TABLES

xiii

CHAPTER I

INTRODUCTION

As the environmental awareness is being raised and knowing the fact that conventional power systems' cost of energy is expected to increase, the need for a new, more environmentally friendly energy system is rising. Several countries are exhibiting transitions from fuel fired centralized electricity generation toward renewable based distributed power generations.

The continuous reduction in renewable system's energy production costs, especially photovoltaic systems [1], made their integration more attractive. Through which their contribution among the total power generated capacity is expected to increase significantly as we reach 2050 [2].

However, renewable sources are intermittent, thus their continuous fluctuations can greatly affect the network's voltage and frequency, and therefore, reduce power quality and reliability. That is why energy storage systems were utilized to cope with such integration and reduce intermittency effects.

As the integration of such technologies, and combining them with the conventional ones, is getting wider, a new energy system was formed. This system is called a microgrid (MG).

A. Defining Microgrids (MG)

Microgrid can be defined as a group of distributed energy resources and interconnected loads with clearly stated electrical limits. Such group acts as a single and controllable entity with respect to the grid. It can operate in both off-grid and grid connected modes as to assure a reliable and economic power supply to its local prosumers. It ranges from two small generators supplying a certain load, to a group of generators supplying power to a university campus, small village, mall or a hospital.

Heavy research studies had been implemented on optimizing microgrids from a sizing, siting and energy dispatch point of view. Such research revealed the significant ability of microgrids to embrace distributed energy resources and improve network's performance, affordability and reliability.

B. Defining Microgrids Community (MGC)

Despite the improvements attained in cost, reliability and sustainability of energy sector, the performance of the microgrid is still hindered due to several limitations such as spatial, economic, technical, etc… Such limitations can be clearly observed when microgrids are operating in islanded mode. Thus, in an attempt to improve the network's performance and making use of the wide integration of distributed energy resources, the idea of forming microgrids community (MGC) was suggested.

The basic principle behind MGC is to supply various loads through distributed energy resources owned by several owners. The objective of such cooperation is to increase the electric services' reliability and resiliency such that optimal economic and societal goals are achieved while satisfying the demand. Similar to MG, MGC not only operate in grid

2

connected mode, but it can also detach from large grids and operate in islanded mode. In order to differentiate MGCs from MGs, MGC is characterized by the following:

1. It must contain at least 2 MGs.

2. MGs in MGC must be owned by different owners, thus each MG has its own operational goals.

3. MGs in MGC must be in closed proximities.

Since "*MGs in MGC must be owned by different owners*", its implementation can't be done without forming a suitable market model governing the exchanged energy among its participants. However, the market model shouldn't only deal with exchanged energy from technical or economic perspective, but it should also account for each MG's security.

The following study will be organized as follows: chapter II provides a literature review about the most recent studies involving microgrids and microgrids community, chapter III describes the problem that this work is tackling, modelling of the entire system is discussed in chapter IV, methodologies and algorithms utilized are discussed in chapter V, results are provided in chapter VI, and finally conclusions and future work are drawn in chapter VII.

CHAPTER II

LITERATURE REVIEW

A. Microgrids

1. Literature Related to Impacts of Implementing Microgrids in Distribution Network

To strike a balance between the effect of intermittent sources and providing reliable form of energy, the need for cost effective energy storage (ES) and energy management systems (EMS) have been the focus of research. For instance, [3] suggested that the problems associated with the integration of non-dispatchable distributed generations can be eliminated by an appropriate battery energy storage system. The approach was based on finding the optimal planning of battery-coupled distributed PV generators (BCDPGs) based on finding its optimal size, location and battery's dispatching strategy that yields minimum energy losses. Results of that study revealed that such implementation was cable of reducing network's energy losses by approximately 41% and voltage deviations by almost 36% while increasing clean energy penetration to approximately 50%. A further study about sizing and allocating of energy storage was conducted in [4], where the study revealed that the optimal storage system configuration achieved significant reduction in the daily cost of energy and in the network's energy losses while accounting for the network's voltage. Similarly, studies done in [5] - [8] discussed the advantages attained due to proper sizing, siting and dispatch strategy of a battery storage system that yields minimum operational cost and power losses while mitigating the impact of voltage fluctuations due to PV penetrations.

2. Literature Discussing Different Optimal Sizing, Siting and Dispatch Approaches

Integer variables, used to decide components' locations or states, and non-convex power flow constraints make the optimal power flow (OPF) problem NP-hard, thus different approaches have been devised to solve such problem and alleviate the computational burdens. Although sizing and siting problems are mostly solved through heuristic approaches, OPF problem is observed to be solved through 2 different approaches: (1) convex approximations and (2) heuristic approach.

Several convex approximations have been made to the OPF problem, where different utilized programming algorithms, such as quadratic and quadratically constrained programming, 2nd order cone programming, semi definite programming etc…, were proven to be an applicable approach [9] – [16].

Similarly speaking significant number of studies were based on utilizing heuristics, for instance, [17] proposed a dual loop optimization method combined with electron drifting algorithm for sizing and dispatching of battery energy storage system (BESS) in distribution grid with photovoltaic (PV) generation. Whereas, [18] and [19] discussed the use of particle swarm optimization (PSO) technique to converge to an optimal battery storage system siting, sizing and dispatch that would minimize energy losses while reaching the desired smoothing power level in distribution networks with renewable generations. Unlike the last-mentioned references, the utilization of PSO in [20], to converge to an optimal real time energy management battery control action of a known battery storage capacity, resulted in a 44.5% reduction in energy cost. [21] – [25] proposed the use of genetic algorithm (GA) optimization approach to converge to an optimal size, site and energy dispatch strategy of distributed energy resources that minimizes energy

losses, voltage fluctuations due to high renewable penetration levels, and operational cost in distribution networks. On the other hand, [26] and [27] demonstrated a multi-objective optimization approach, also solved through utilizing GA, for optimal sizing and siting of energy storage systems in distribution networks. The former study was aimed to reduce peak power and energy losses while minimizing the investment cost, whereas the latter accounted for energy losses, investment cost and carbon emissions.

All of the previously mentioned studies, plus plenty more, had revealed how "Microgrids" can effectively embrace distributed energy resources (DERs) in distribution networks (DNs) and address the associated energy economic issues by making electricity grid smarter through optimal DERs' configurations and optimal energy management schemes. However, despite the great results observed, network's reliability is still questioned. For instance, the study made in [28], showed that although the optimal operation strategy of a hybrid PV-Battery system resulted in energy cost reduction and improved reliability, it still fails to secure 100% demand coverage under grid blackouts. Therefore, it's obvious that when a single MG operates in islanded mode, the reliability of satisfying its local demand is hindered due to financial, spatial and technical limitations on the DERs' capacities installed.

B. Microgrids Community (MGC)

As the number of microgrids is increasing and as a proposed solution to enhance the network's reliability, the concept of "Microgrids Community" (MGC) was introduced. MGC is achieved through connecting MGs in close geographical proximity, leading to

further improvements in the network's reliability, especially during islanded mode, through energy scheduling and reciprocity among these MGs.

The main difference between simulating a MG and an MGC is the need for an appropriate market model. Most of the MG's optimization scenarios were based on DERs owned by a single party and the focus was on reducing the MG's daily operational cost and maintaining a good quality electricity. However, MGC is a group of MGs and each one is owned by a different owner; thus, each prosumer seeks his/her own benefit. Therefore, the need for a market model that satisfies all MGs is essential for developing an active MGC.

Several studies focused on MGCs and different markets and dispatching criteria were discussed in the literature. For instance, [29] proposed the use of a game-theoretic model for a peer-to-peer (P2P) energy trading market between prosumers within a community. The authors separated such modelling into two separate competitions. The first one represents the price competition among the sellers which was modelled as a non-cooperative game. While the second one represents the seller selection competitions among the buyers where evolutionary game theory was utilized. When comparing the results of the proposed market model to the results of a peer-to-grid model, significant reduction in cost was observed for all participating peers. Game theory was also adopted in [30] which proposed a 3-dimensional system architecture for the modelling of a P2P energy trading market through utilizing non-cooperative bidding. The 1st dimension was divided into 4 layers containing the physical components layer, communication layer, control layer and the business layer. Whereas the 2nd and 3rd dimensions described the size of peers participated and the time sequence of the P2P energy trading process respectively. The implementation of the proposed approach yielded significant reduction: (1) in the

exchanged power between a microgrid and the utility grid and (2) in the peak demand observed by the utility grid, thus reducing grid dependency. Also utilizing game theory, reference [31] demonstrated the use of a hybrid multi-leader (sellers) multi-follower (buyers) Stackelberg game and a minimizing consumers' bill and carbon emissions. Reference [32]-[33], on the other hand, proposed another P2P market model based on allowing surplus energy to be shared between prosumers in a neighborhood. The energy requirement of the community was performed through an aggregated small-scale battery control system. The objective of such energy management system was to maximize the community's energy self-consumption, thus reducing grid's dependency and minimizing the energy cost of the entire community. Upon comparing the proposed P2P model with the P2G model, results revealed the formers superiority over the latter through which energy self-consumption increased by approximately 30% with a 34% reduction in the community's energy cost. A different market model illustrated in [34] utilized a two-step approach to develop an energy market operating in a grid. The first one utilized dynamic programming (DP) in order to perform an economic dispatch for each agent within the grid which were used to derive the bids. Whereas the second one dealt with the market behavior aiming to calculate the electricity spot price during each hour. Market clearing price was found by the market operator through achieving load generation balancing. Unlike others, reference [35] discussed the implementation of an open market business model among multiple stakeholders to develop the basics of a future flexible retail energy market in community microgrids. Different pricing strategies (Time of Use (ToU), Feed in Tariff (FIT), and Fixed Price (FP)) were combined in the market model such that each DER owner may sell power to the community microgrid either on FIT, FP or as per ToU.

Similarly, each customer is assumed to have an opportunity for a reliable and a cost-effective supplier selection. Utilizing GA to decide on the hourly dispatch, the results revealed that all stakeholders had the advantage of participating in such market. Whereas the revenues attained by the grid decreased slightly, since that amount of power purchased from the grid is now supplied by one of the stakeholders. Authors in [36] suggested the use of blockchain-assisted distributed double auction trading platform to facilitate the P2P trading between prosumers in a LV network. The proposed methodology was tested on an unbalanced 3 phase European LV network, where results revealed that a moderate level of P2P trading doesn't have a significant influence on the network's performance, since upon implementing the proposed approach, insignificant variations were observed in phase voltage unbalance rate and active power losses as compared with the base scenario. The use of blockchain for decentralizing transactive energy management was also analyzed in [37] to guarantee a secure, scalable and efficient market. Authors in [37] had reached to a conclusion assuring that blockchain technologies embedded in transactive energy will play a vital role in the transition toward an active distribution network. Reference [38] proposed a timely discrete sealed double-sided auction to govern energy transactions between sellers and buyers in a distribution network. The implementation of the proposed approach resulted in: (1) an increase in self-consumption of the network and (2) a 23% reduced energy costs. Reference [39] investigated the impacts of optimizing rooftop photovoltaic distributed generations with battery storage under P2P energy trading platform. Mixed integer linear programming was utilized in order to minimize the net cost of the community, where the results revealed savings up to 28% for households equipped with large photovoltaic systems and battery storages. However, results also revealed that

9

households with photovoltaic systems have lower savings during excessive PV penetration, due to their low price and its impact on the lowering market clearing price. A two-stage stochastic bidding optimization strategy for microgrid energy market participation is proposed in [40]. The first stage dealt with optimizing the bidding strategy in the day-ahead market, whereas in the second stage, and according to the market clearing results, the MG re-optimizes its power generation plan in order to further reduce its daily cost.

Unlike the previously mentioned literature [41] provided a thorough description of MGCs, as well as a hierarchical energy management system controlling the MGC without diving into a detailed market model. The authors in [41] divided the energy management system controlling the MGC into a two-level hierarchical approach. The lower level, to be executed first, focuses on individual MGs, where it optimizes the power output of MGs' dispatchable units and the exchanged power with the upper network. Whereas the upper level, takes the lower level's results as constraints and decides on the microgrid community level devices' (MCLDs) dispatch and the exchanged power between MGs. The proposed methodology was tested under 4 different operating scenarios, where results revealed the superiority of the scenarios during which the MGC was operating under interconnected mode.

CHAPTER III

PROBLEM FORMULATION

The literature provided in chapter II reveals the ability of MGs to embrace distributed energy resources and significantly improve the network's performance economically and technically. As can be observed from the provided literature, most studies were performed to deduce the benefits of optimizing a microgrid either operating under a reliable grid operation or in islanded operation. However, very few studies, as per the author's knowledge, discussed the operation of a microgrid under grid blackouts, as the case in developing countries. Similarly, when MGC's performance was studied and different market models were tested, none of the literature studies developed a market model suitable for developing countries were the grid is unreliable, and DERs might not be able to cover the entire network's demand as the case in [28].

The study performed in [28] had revealed an important limitation of a MG. Despite the significant reduction in the total daily hours of power loss, it wasn't able to assure a continuous power supply due to several reasons (cost and available spaces). Needless to mention, such results were attained for a residential load, but what would be the case if it was a critical load such as hospitals, pharmacies, schools, university campuses, malls or other major loads that affect the society. Obviously, due to spatial, economic and environmental limitations, MGs might fail providing a reliable and a continuous power supply to such loads.

Therefore, this study aims first to test the applicability and attractiveness of implementing DERs in distribution networks operating under unreliable grid. Then study the influence of building a suitable decision-based day ahead market mode on the distribution network's performance.

An IEEE 123 bus test feeder is taken to be the platform for such implementation, where it will be divided into 24 light loads and 6 major MGs (3x residential microgrids (RMGs), a hospital, a mall and a university campus). Initially, the distribution network is assumed to be supplied by an unreliable grid and private sectors' diesel generators (DG) with limited capacities.

The first task will deal with optimizing the performance of each of the 6 MGs through converging to an optimal photovoltaic (PV) and battery storage system (BSS) configurations (only for hospital, mall and university campus) along with a suitable energy management system that aims to supply 100% reliable source of energy with the least possible operating cost and diesel dependency.

The second step aims to develop a suitable decision-based day ahead market model that tests the attractiveness of allowing MGs to exchange energy among themselves. Comparison between both operations will be done based on discussing the technical, environmental and financial merits achieved in both operating scenarios.

CHAPTER IV

SYSTEM MODELLING

Modelling the entire system is illustrated through a three-dimensional architecture as depicted in figure 1. The first dimension involves the key functions of the modelled distribution network and consists of 4 layers. The distribution network's physical layer is the first layer. This layer contains all components found in the distribution network including feeders, loads, distributed energy resources, smart meters, etc… The second layer is the information and communication technology which consists of communication devices, protocols and information flow. The control layer is the third layer which mainly describes the strategies for preserving high-quality and reliable power supply while adjusting the actual exports to be the same as the scheduled ones. Such layer contains load control, frequency control, voltage control etc... The fourth and last layer is the energy market layer. This layer defines the energy market participants and illustrates the trading strategy process among them. The second dimension, in the proposed system's architecture, categorizes loads and distributed energy resources in the distribution network based on their size. While, the third and last dimension, organizes the time sequence of the proposed energy trading market model. This layer organizes bidding process, energy trading agreements, energy exchanging and settlement processes.
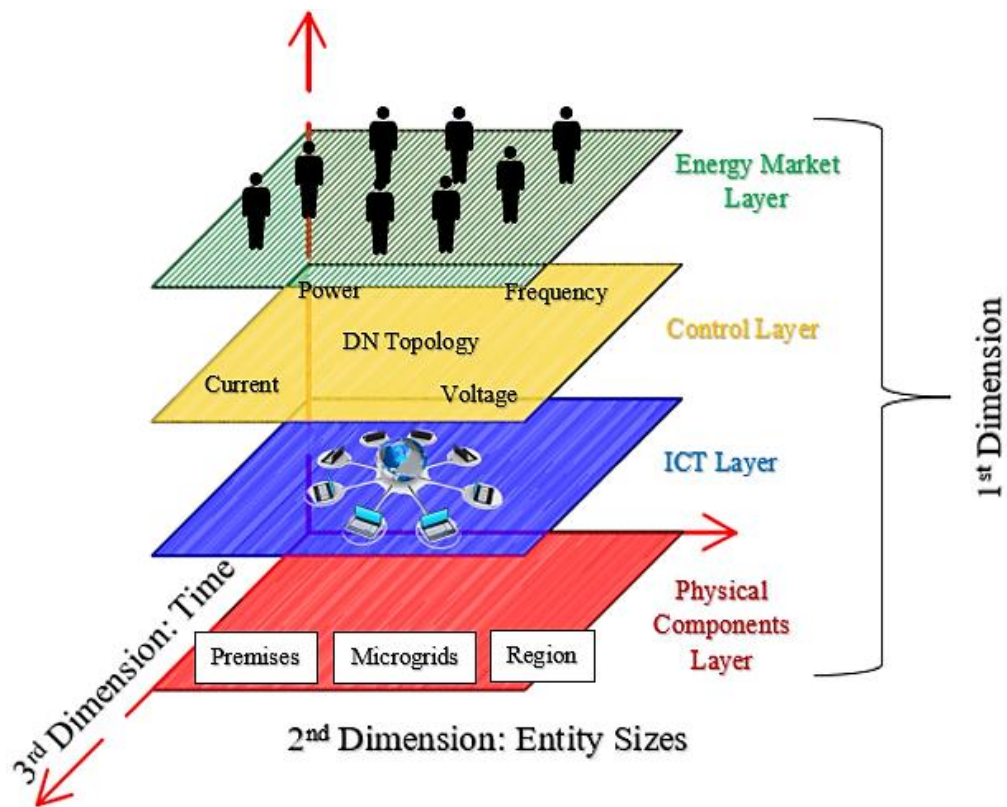
Fig. 1: System's architecture

A. 1st Dimension

1. Physical Components Layer

a. <u>IEEE 123 Bus Distribution Network</u>

The IEEE 123 distribution network is selected to be the platform of the suggested study. However, to serve the paper's objective and for simplicity, few modifications were made to the original IEEE 123 test feeder such that switches, transformers and capacitor banks were removed and a main switch was added to the distribution network to represent the fact that such network is supplied by an unreliable grid characterized by blackouts as

shown in figure 2. Also, for simplification, the network is assumed to be perfectly balanced

and connected through underground cables having the characteristics shown in table 1.
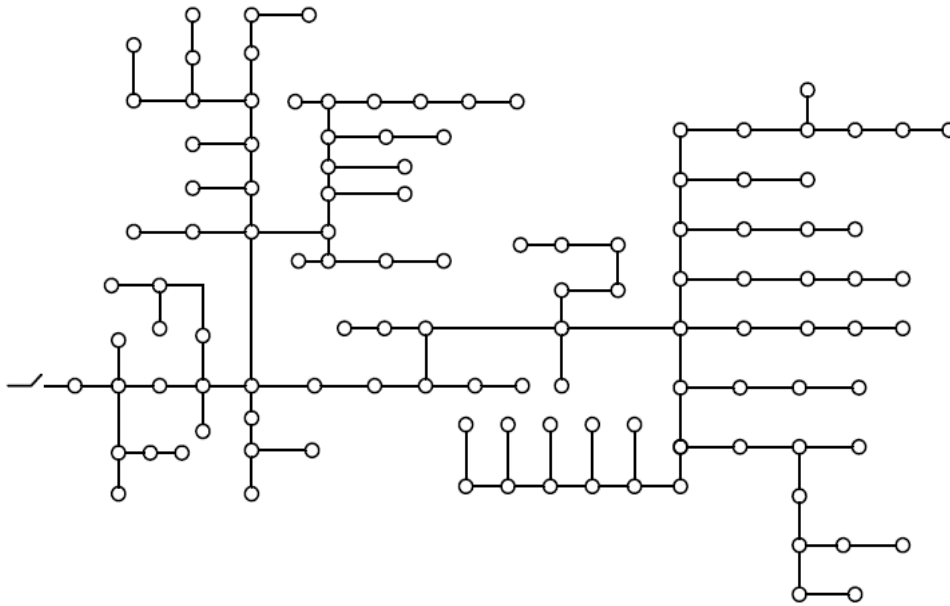
Fig. 2: Modified IEEE 123 distribution network

Table 1: Distribution network's cables characteristics

r (Ω/mile)	x (Ω/mile)	b (μs/mile)
1.521	0.752	67.22

b. <u>Grid Modelling</u>

The distribution network is assumed to operate under an unreliable grid

characterized by scheduled daily blackouts. The grid's assigned energy outage is set to 3

hours a day. Daily scheduled outage occurs at certain periods as shown in table 2.

Table 2: Scheduled daily grid's outage

Blackout Timing # 1	07:00 am to 10:00 am
Blackout Timing # 2	10:00 am to 13:00 pm
Blackout Timing # 3	13:00 pm to 04:00 pm
Blackout Timing # 4	04:00 pm to 07:00 pm

However, although blackouts are assumed to be scheduled, there still exist the possibility of unpredicted daily blackouts or even no blackouts to occur. A pie chart depicting the frequency of grid's outage based on its daily duration is provided in figure 3.

Grid's Daily Blackout Frequency
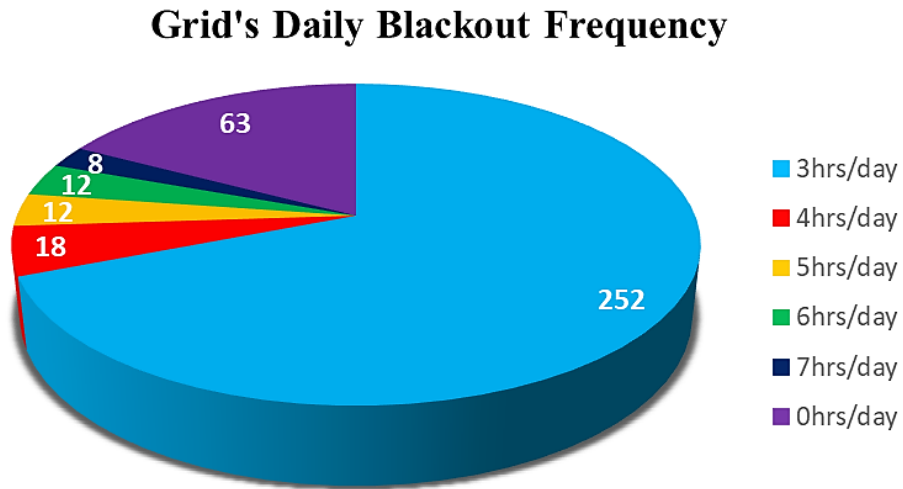
Fig. 3: Grid's daily blackout frequency based on its daily duration

Two different grid tariff rating schemes are adopted in this study. Loads representing university campus, mall and hospital are subjected to a triple tariff rate scheme. Whereas,

light and residential loads are subjected to a fixed grid tariff rate. Both tariff rate schemes

adopted are shown in table 3.

Table 3: Grid's tariff rates schemes

	Triple Tariff Rates	Fixed Tariff Rate
Night Tariff	0.053 $/kWh	
Mid-day Tariff	0.073 $/kWh	0.133 $/kWh
Peak Tariff	0.213 $/kWh	

In order to model grid blackouts, a binary operator (Λ) will be assigned to the power

supplied by the grid, such that when Λ is high (1), the grid is ON and when Λ is low (0),

the grid is OFF. Therefore, the grid output power will be represented using the following

equation:

$$P^{Grid}(t) = \Lambda(t) \times P_G(t) = \begin{cases} P_G(t) & for\ \Lambda = 1 \\ 0 & for\ \Lambda = 0 \end{cases} \tag{1}$$

Where $P^{Grid}(t)$ is the power supplied (in kW) by the grid at any time t and $\Lambda(t)$ is a binary

operator that represents the grid state at any time t.

c. <u>Diesel Generator Modelling</u>

The presence of a reliable and dispatchable electric power source, in the absence of reliable grid, is essential in any hybrid power system. Since the grid under study, is characterized by scheduled blackouts, diesel engine generators are considered to be available to enhance the network's ability to compensate for energy outage.

Modelling diesel generators requires the following information: diesel generator's capital cost, diesel fuel price, diesel generator's rated power, diesel generator's fuel consumption and its operation and maintenance cost [42] [43] [44]. Once obtaining such info, the following set of equations can be used to model the diesel generator set:

$$FC(t) = \alpha\, P_{Dg}(t) + \beta P_{Dg,rated} \tag{2}$$

$$C_F(t) = FC(t) \times \psi(t) \tag{3}$$

$$CC^{DG} = f(P_{Dg,rated}) \tag{4}$$

$$OM^{DG} = f\left(\sum_{t=t1}^{T} P_{Dg}(t)\right) \tag{5}$$

$$CRF(i, N) = \frac{i \times (1+i)^N}{(1+i)^N - 1} \tag{6}$$

$$AP^{DG} = CC^{DG} \times CRF(i, N) + OM^{DG} \tag{7}$$

$$COE^{DG} = \frac{AP^{DG}}{\sum_{t=t1}^{T} P_{Dg}(t)} \tag{8}$$

Where, FC is the fuel consumption (in L) at time t, P_{Dg} and $P_{Dg,rated}$ are the actual

output power and rated power of the diesel generator respectively (in kW), α and β are fuel

consumption coefficients, CF is the diesel fuel cost of the diesel generator (in $) at time t

and \psi is the diesel cost (in $/L) at time t. CC^{DG} and OM^{DG} are diesel generator's capital

cost and operation and maintenance cost (in $). CRF is the capital recovery factor at an

interest rate "i" for an "N" period loan, AP^{DG} is the annual payment (assuming that capital

cost is fully covered through a bank loan) and COE^{DG} is the diesel generator's cost of

energy (in $/kWh).

d. Photovoltaic Modelling

PV output can be modelled using the following equations 9 to 22 [45] [46]

[47][48]:

$$P_{PV,AC}(t) = PVout(t) \times \eta_{inv} \tag{9}$$

$$PVout(t) = FF(t) \times Isc(t) \times Voc(t) \tag{10}$$

$$Isc(t) = \frac{S}{S_{STC}} \left[I_{sc,STC} + K_i(Tc(t) - 25) \right] \tag{11}$$

$$Voc(t) = V_{oc,STC} - K_v \times (Tc(t) - 25) \tag{12}$$

$$FF(t) = FF_0(t) \times [1 - r_s(t)] \tag{13}$$

$$FF_0(t) = \frac{V_{oc,0}(t) - \ln[V_{oc,0}(t) + 0.72]}{V_{oc,0}(t) + 1} \tag{14}$$

19

$$V_{oc,0}(t) = Voc(t) \times \frac{q}{nk[Tc(t) + 273.15]} \tag{15}$$

$$r_s(t) = R_s \frac{Isc(t)}{Voc(t)} \tag{16}$$

$$Tc(t) = Ta(t) + s \frac{NOCT - 20}{0.8} \tag{17}$$

$$R_s = R_{s,STC} = r_{s,STC} \frac{V_{oc,STC}}{I_{sc,STC}} \tag{18}$$

$$r_{s,STC} = 1 - \frac{FF_{STC}}{FF_{0,STC}} \tag{19}$$

$$FF_{STC} = \frac{V_{mppt,STC} \times I_{mppt,STC}}{V_{oc,STC} \times I_{sc,STC}} \tag{20}$$

$$FF_{0,STC} = \frac{V_{oc,0,STC} - \ln[V_{oc,0,STC} + 0.72]}{V_{oc,0,STC} + 1} \tag{21}$$

$$V_{oc,0,STC} = V_{oc,STC} \times \frac{q}{nk[Tc_{STC} + 273.15]} \tag{22}$$

Where, $P_{PV,AC}$ is the AC output power (in kW), PVout(t) is the maximum output power (in kW) at any time t, η_{inv} is inverter efficiency, Isc(t) and Voc(t) are the short circuit current (in Amps) and open circuit voltage (in Volts) under operating conditions, s is the solar irradiance (kW/m2) at any time t, FF and FF_0 are the actual and ideal fill factor of the module, $V_{oc,0}(t)$ is the normalized open circuit voltage at any time t, q is the charge of an electron, n is the ideality factor assumed equal to 1, k is Boltzmann's constant, Tc(t) is the module's temperature at any time t (in ˚C), Rs is the module series resistance, $r_s(t)$ is the normalized module series resistance at any time t, Ta(t) is the module ambient temperature (in ˚C) and NOCT is the nominal operating cell temperature (in ˚C) provided by the

manufacturer. "$r_{s,STC}$" is the normalized series resistance under standard test conditions (STC), FF_{STC} and $FF_{0,STC}$ are the actual and ideal fill factor under STC respectively and $V_{oc,0,STC}$ is the normalized open circuit voltage under STC.

To calculate the hourly output of the PV system, hourly measurements of solar irradiance and ambient temperature must be provided. Figures 4 and 5 illustrate the annual temperature and irradiance profiles respectively. Using the PV module characteristics, provided in table 4, and the set of equation (9)-(22), the output power of the PV module selected is shown in figure 6.
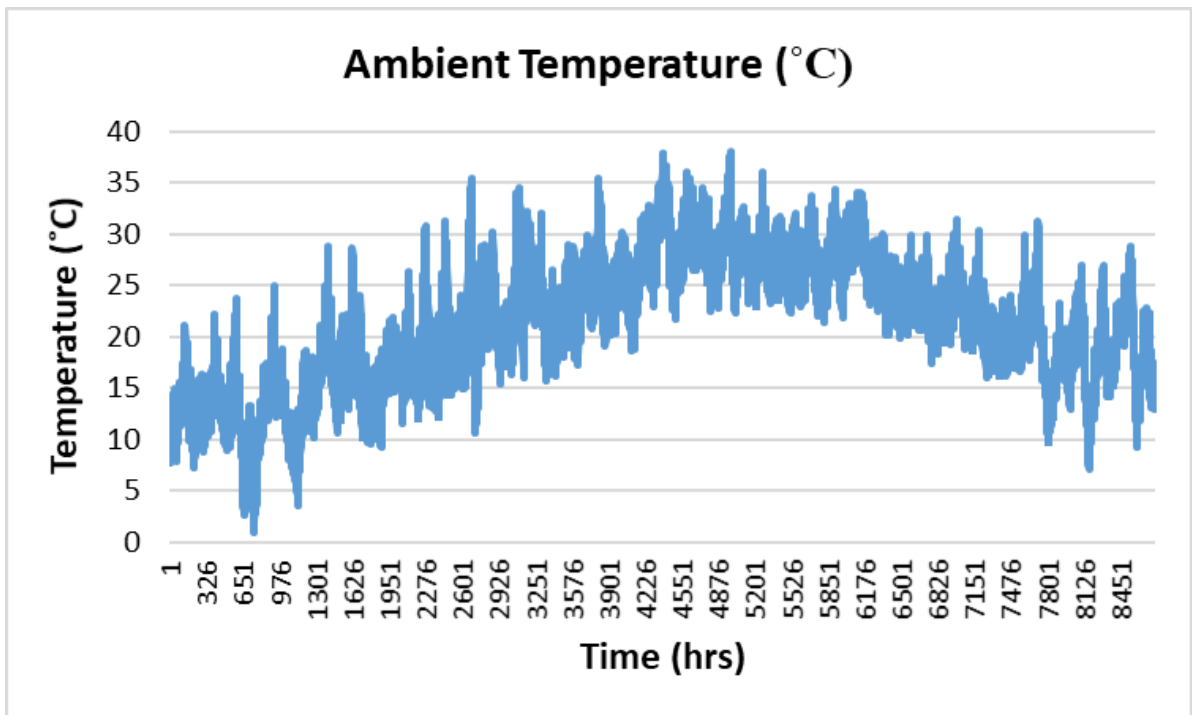
Fig. 4: Ambient temperature annual profile
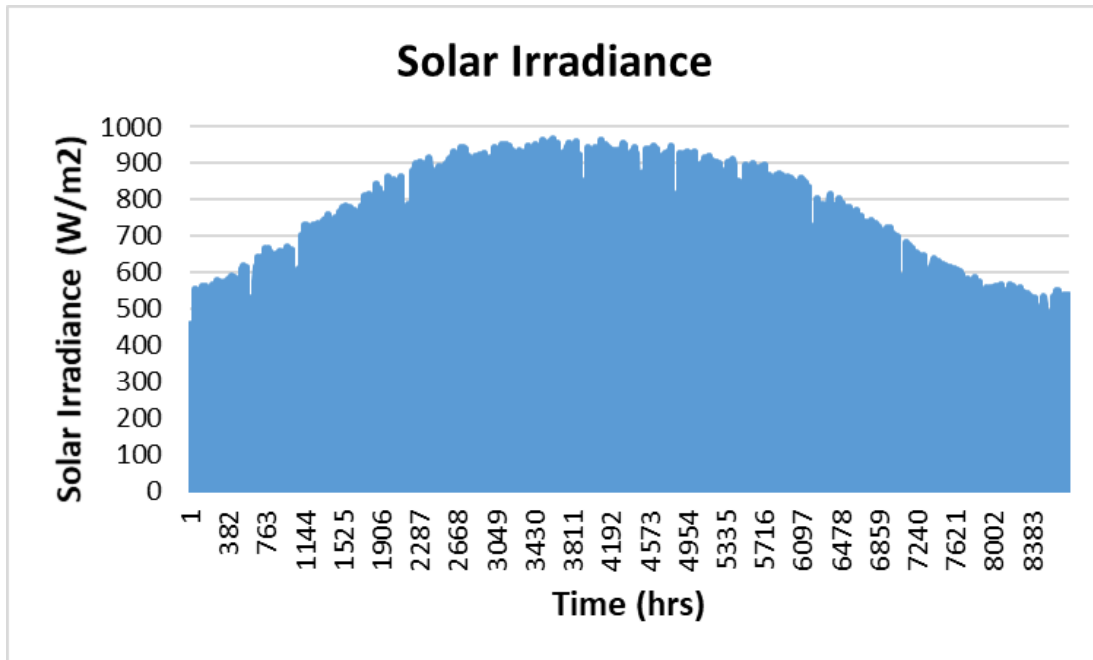
Fig. 5: Solar irradiance annual profile

Table 4: PV module characteristics [49]

LG365Q1C-A5	
Voc,STC (V)	42.8 V
Isc,STC (A)	10.8 A
Vmppt, STC (V)	36.7 V
Imppt, STC (A)	9.95 A
NOCT (˚C)	44 ˚C
Kv (V/˚C)	-0.10272 V/˚C
Ki (A/˚C)	4.00E-03 A/˚C
Dimensions (mm3)	1700 x 1016 x 40
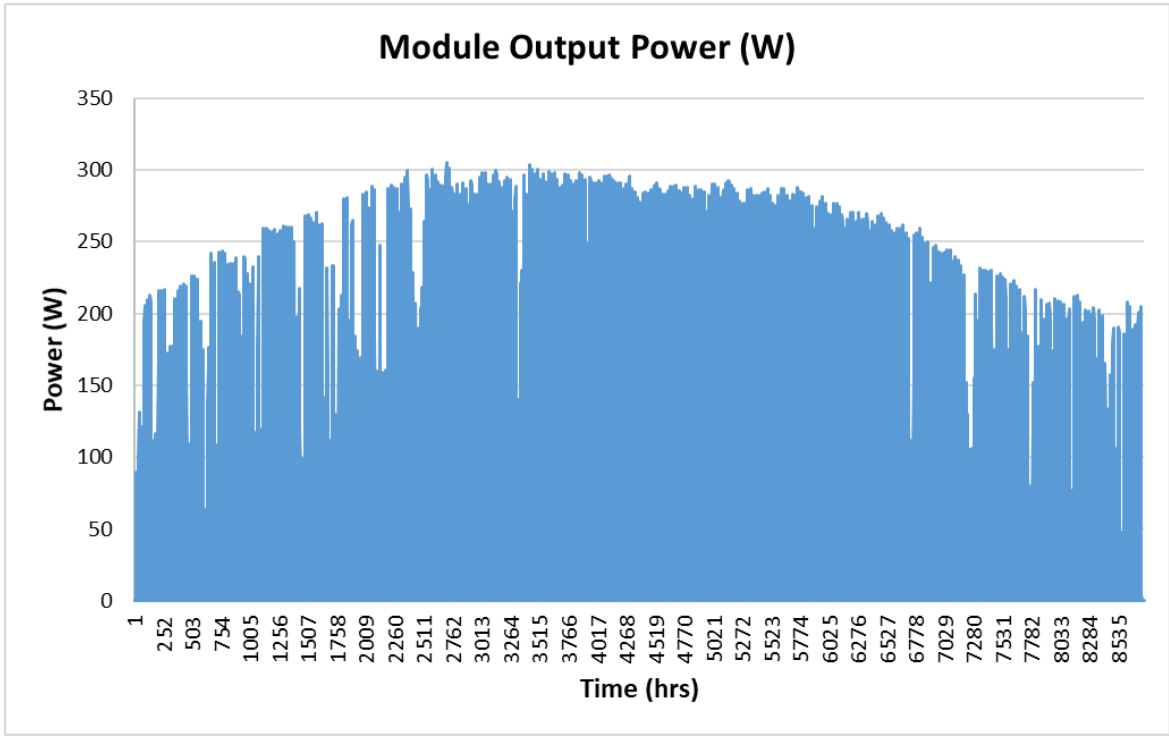
Fig. 6: PV module annual output power profile

PV's financial modelling is illustrated in the following set of equations (23)-(26):

$$CC^{PV} = f(P_{rated}^{PV}) \tag{23}$$

$$OM^{PV} = f(P_{rated}^{PV}) \tag{24}$$

$$AP^{PV} = CC^{PV} \times CRF(i, N) + OM^{PV} \tag{25}$$

$$COE^{PV} = \frac{AP^{PV}}{\sum_{t=t1}^{T} P^{PV}(t)} \tag{26}$$

Where, P^{PV}_{rated}, CC^{PV}, OM^{PV}, AP^{PV}, and COE^{PV} are PV system's rated capacity (in kW), capital cost (in $), operation and maintenance cost (in $), annual loan payment (in $) and cost of energy (in $/kWh) respectively.

e. Battery Storage System Modelling

Equations 27 to 33 are used to model the battery storage system [52].

$$P^{BSS}_{AC}(t) = \begin{cases} \dfrac{P^{BSS}_{DC}(t)}{\eta^{BSS}} & Charging \\ P^{BSS}_{DC}(t) \times \eta^{BSS} & Discharging \end{cases} \tag{27}$$

$$P^{BSS}_{DC(t)} = \frac{E^{BSS}(t) - E^{BSS}(t - \Delta t)}{\Delta t} \tag{28}$$

$$SOC(t) = \begin{cases} SOC(t - \Delta t) \times (1 - a) + \eta^{BSS} \dfrac{P^{BSS}_{AC}(t)}{C^{BSS} \times V \times SOH(t)} \Delta t & Charging \\ SOC(t - \Delta t) \times (1 - a) + \dfrac{P^{BSS}_{AC}(t)}{\eta^{BSS} \times C^{BSS} \times V \times SOH(t)} \Delta t & Discharging \end{cases} \tag{29}$$

$$CC^{BSS} = f(P^{BSS}_{rated}) \tag{30}$$

$$OM^{BSS} = f(P^{BSS}_{rated}) \tag{31}$$

$$AP^{BSS} = CC^{BSS} \times CRF(i, N) + OM^{BSS} \tag{32}$$

$$COE^{BSS} = \frac{AP^{BSS} + \sum_{t=t1}^{T} P^{BSS}_{char}(t) \times \varphi}{\sum_{t=t1}^{T} P^{BSS}_{disch}(t)} \tag{33}$$

Where, E_{batt} is the battery energy (in kWh), $P_{DC}^{BSS}(t)$ is the DC charging-discharging rate of the battery (in kW) in an interval Δt. $P_{AC}^{BSS}(t)$ is the AC power to charge or discharge from the battery (in kW) with a battery-inverter efficiency η^{BSS}. SOC(t)

is the state of charge of the battery, C^{BSS} is the nominal battery capacity (in Ah), V is the battery nominal voltage (Volts), "a" is the self-discharging factor, SOH is the batteries state of health. Whereas, P^{BSS}_{rated}, CC^{BSS}, OM^{BSS}, AP^{BSS}, and COE^{BSS} are battery's capacity (in kW), capital cost (in $), operation and maintenance cost (in $), annual loan payment (in $) and cost of energy (in $/kWh) respectively. Whereas, P^{BSS}_{char}, P^{BSS}_{disch} and φ are the charging power, discharging power and charging cost rate respectively.

The data in table 5 provides the state of health relation as a function of discharged energy. In order to account for the impact of energy discharge on the batteries' capacity, a segmented linear function representing SOH as a function of discharged energy is used to describe the batteries' energy retention during the first 10 years.

Table 5: Battery's annual retention regime

Year	Aggregated Discharge (kWh/year/kWh)	Minimum Retention	Yearly Energy Output
1	348	95%	348
2	679	91%	331
3	996	88%	317
4	1302	83%	306
5	1599	79%	297
6	1889	77%	290
7	2173	75%	284
8	2451	73%	278
9	2725	71%	274
10	2994	70%	269

2. Information Communication Layer

A reliable and decent communication system is essential for building a complete system architecture. The implementation and associated technology of such system is beyond the scope of this study. However, this study is based on assuming the presence of a fair communication system, where all prosumers have equal chances to participate in a fair energy market without actually worrying about providing any credential information thus risking the prosumer's security. A detailed description on how the proposed approach tries minimizing the risks on participants' security is provided in energy market layer.

3. Control Layer

Building the control layer algorithm is also beyond the scope of this paper. However, the success of the proposed system architecture cannot be achieved without a reliable control system. The control system is a vital block in the proposed system's architecture since it is responsible of:

1. Controlling the dispatchable units to oblige to the dispatch strategy decided.

2. Providing ancillary services in the distribution network, such as regulating the network's frequency, mitigating voltage fluctuations and restricting them to the normal operating band.

3. Guaranteeing appropriate operation of all physical components under its supervision.

4. Energy Market Layer

Countless studies employed a peer to peer energy market model, where each participant has the choice to select a suitable energy supplier. As demonstrated in the literature review, peer to peer energy market showed great potential in enhancing the distribution network's reliability and increasing the participants' profits through exchanging energy with other peers. However, and as per author's personal opinion and for several reasons, peer to peer energy market isn't suitable for developing countries yet. First of all, most of the literature reviews, who utilized peer to peer market model, based their studies on the presence of reliable supplier(s). However, this study is based on their absence. Second of all, energy pricing was made based on knowing the external energy market price. However, as is the case in many developing countries, there is one party that is responsible for supplying energy, and it is unreliable, thus there is no external market. Last but not least, most of the market models aimed to find the optimal dispatch strategy and energy pricings that maximize the parties' profits and minimize the consumers' expenses. However, this paper mainly focuses on developing a suitable energy market that enhances the network's reliability and reduces its diesel and grid's peak energy dependency in first place, while accounting for parties' profits in second place. Hence, to avoid the above-mentioned obstacles, this paper suggests the utilization of a decision-based day-ahead pool-based energy market.

Pool energy market is a centralized marketplace where participants submit their bids and offers for the amount of energy, they are willing to buy or sell. Although each participant may set his/her own unique energy price, energy is exchanged, during a certain

interval, at a single spot price called "market clearing price" assigned by a 3rd party

member. Then, the proposed market model consists of three unique market participants

interacting in the pool energy market as depicted in figure 7. These three participants are:

(1) distributed system operator (DSO) representing the unreliable grid, (2) microgrid

community agent (MGCA) acting as an auctioneer and a community optimizer and (3)

microgrid/load agent (MG/LA) acting as prosumers (producers and consumers of energy).
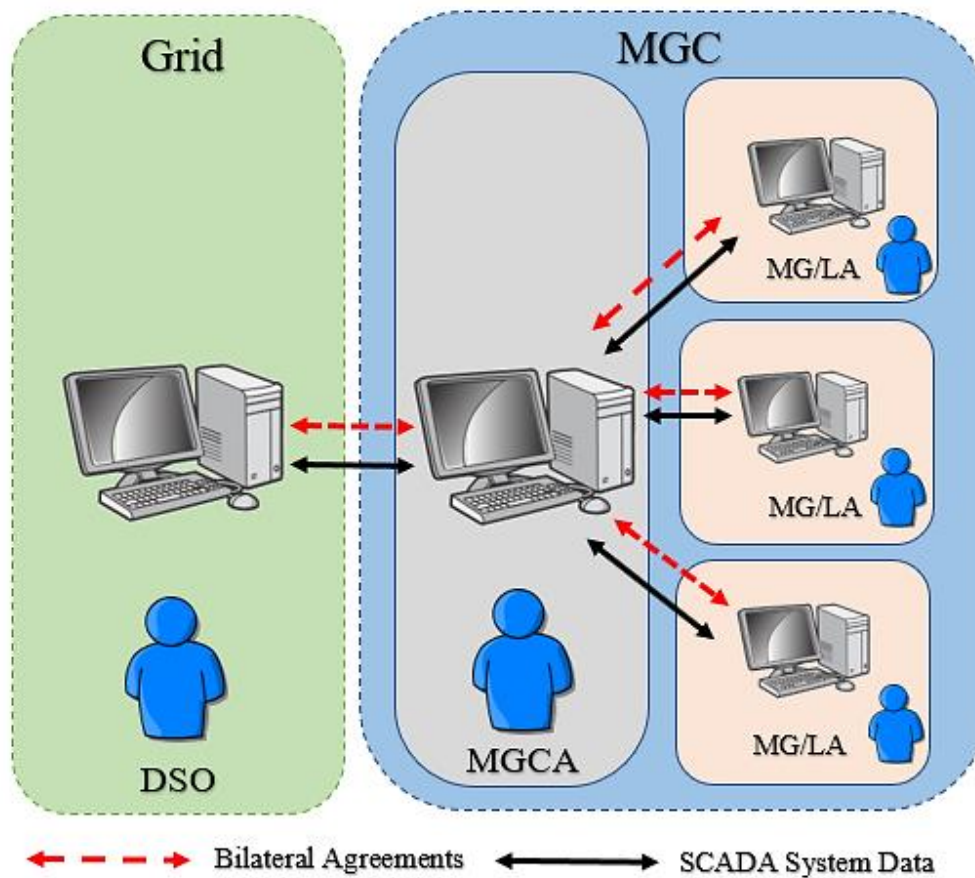
Fig. 7: Market model architecture

a. Distributed System Operator (DSO) Role

The DSO is the first player in the proposed energy market model. He is the gatekeeper responsible of maintaining decent operation of the entire distribution network through accepting or declining the energy transaction scheme, provided by the MGCA, such that none of the distribution network's technical constraints are violated.

DSO participates on behalf of the grid in the wholesale market, thus he plays a vital role in striking balance between generation and demand and in providing the MGCA with the upcoming grid's daily blackout schedule, such that the MGCA will have full knowledge of the grid's state for the upcoming day.

Another task to be fulfilled by the DSO is reaching an acceptable agreement with MGCA regarding the charges (in $/kWh) assigned on using the distribution network as an energy pool among different parties. However, for problem cost simplification, this task was not considered in this work.

b. Microgrid Community Agent (MGCA) Role

The MGCA is the second and most important player in the proposed market model. He is the link between MG/LAs and the DSO and he is considered to be the brain of the entire community.

In the proposed market model, MGCA is a non-profit entity with no generating capacities nor load requirements. Thus, MGCA acts as an independent participant, that is capable of deploying a collusion free energy market, providing all players with equal

opportunities to benefit from market participation. Unlike a regular auctioneer responsible only of clearing the market through calculating energy spot prices, MGCA, in the proposed market, is responsible of using the generation capacities with its assigned bidding prices and load requirement profiles provided by MG/LAs along with the information provided by the DSO for the upcoming day, to come up with an optimal dispatch strategy that minimizes the distribution network's operational cost while focusing on diesel dependency and grid's peak hours purchased energy reduction.

After configuring the optimal dispatch strategy for the upcoming day market window, the MGCA sends it to the DSO for validity test. Once DSO's approval is granted, the MGCA announces the hourly spot market price profile, sends each MG/LA its own private dispatch profile and then wait to receive all MG/LAs participation decisions. If all approved, the market for the upcoming day is closed and participants wait for the exchanging process to start.

However, if some parties denied such dispatch, the energy market enters phase 2, where the MGCA strives to divide market participants into groups based on several considerations, for instance, size of the entity, its characteristics and/or its influence on the welfare of the entire community. Thus, the distribution network is divided into several market pools each having its own market spot price. In a similar manner, MGCA looks for the optimal dispatch strategy, utilizing the provided capacities by each pool, that minimize its corresponding pool market operational cost, sends it to the DSO for approval and then sends it back to each pool participant along with announcing the energy spot price profiles of each.

If all parties within the same pool agreed, then the market negotiations combining these parties for the upcoming day closes waiting energy exchange period to start. Whereas, for market rejecting parties, the MGCA sends a "No-Market" sign to that pool parties, informing them to operate solely during the upcoming day.

Focusing on the bases of the proposed market model and the interaction schemes among its members, it reveals that none of the DERs' owners is actually forced to provide any highly secure information regarding their own microgrids' generating capacities and their actual costs of energy. In the suggested market, even the MGCA will not be provided by the actual generating capability of each owner nor his/her actual generation cost. On the contrary, MGCA will base his/her optimization on the bidding prices and generation capacity that each DERs owner is willing to submit. Hence, not even the DERs' owners have access to such information concerning other owners.

On the other hand, the way the market is configured, none of the suppliers have the upper hand in controlling the market. Since submitting high selling prices will automatically lead to other buyers' loss of interest in market participation, thus failing to sell any of that energy. While reducing the energy selling price might actually increase other parties' interest, since the energy selling price is lower than their actual generation cost of energy.

In addition, an extra role played by the MGCA is a demand side management role. MGCA must also organize the charging process of the batteries without allowing for new peaks to be observed by the grid during charging times. To do so, agreements must be signed between MGCA and MG/LAs. Such agreement illustrates that MG/LAs are willing

to restrict their charging process (time and charging power) to the profile assigned by the MGCA. Whereas, MGCA must ensure that each MG/LAs will receive its required charging energy before its next usage. Otherwise, MGCA must declare uncontrollable charging process during the upcoming day, thus allowing each MG/LA to act on its own.

Moreover, MGCA is also expected to guarantee the network's stability and reliability during grid-off times, through ensuring the presence of a party capable of providing the network's ancillary services. Thus, based on the day ahead generating capacities provided by each MG/LA, MGCA must assign the party with the highest dispatch capability and minimum cost of energy to play the role of the backup or the slack thus providing the network with its ancillary services (frequency regulation, voltage regulation, etc…).

c. Microgrid/Load Agent (MG/LA) Role

Microgrid/Load agents (MG/LA) are the third and last players in the proposed market model. They are the ones controlling the local dispatch of their distributed energy resources and the ones to decide whether to cooperate among themselves or operate on their own. As any prosumer, the main interest of such party is to make profit and reduce its daily energy cost. Therefore, unlike MGCA, each MG/LAs know the exact cost of generation of each unit its locally dispatching. Thus, after receiving the suggested dispatch profile from the MGCA, each MG/LA will calculate the exact daily energy cost, and then reply with approval or rejection.

In the proposed market, each MG/LA must provide the amount of energy its willing to put under the MGCA's disposal, its associated offer and its hourly forecasted load profile during the upcoming day. However, when submitting the energy capacities to the MGCA, each MG/LA must differentiate between the clean energy share and the diesel generator energy share along with their respective selling costs. Through following such approach, each MG/LA can guarantee that none of the confidential information regarding his own unit is at risk of exposure, since no one, not even MGCA, knows the actual financial and technical data of his own dispatchable units. A summary of the proposed market energy trading process is presented in figure 8.
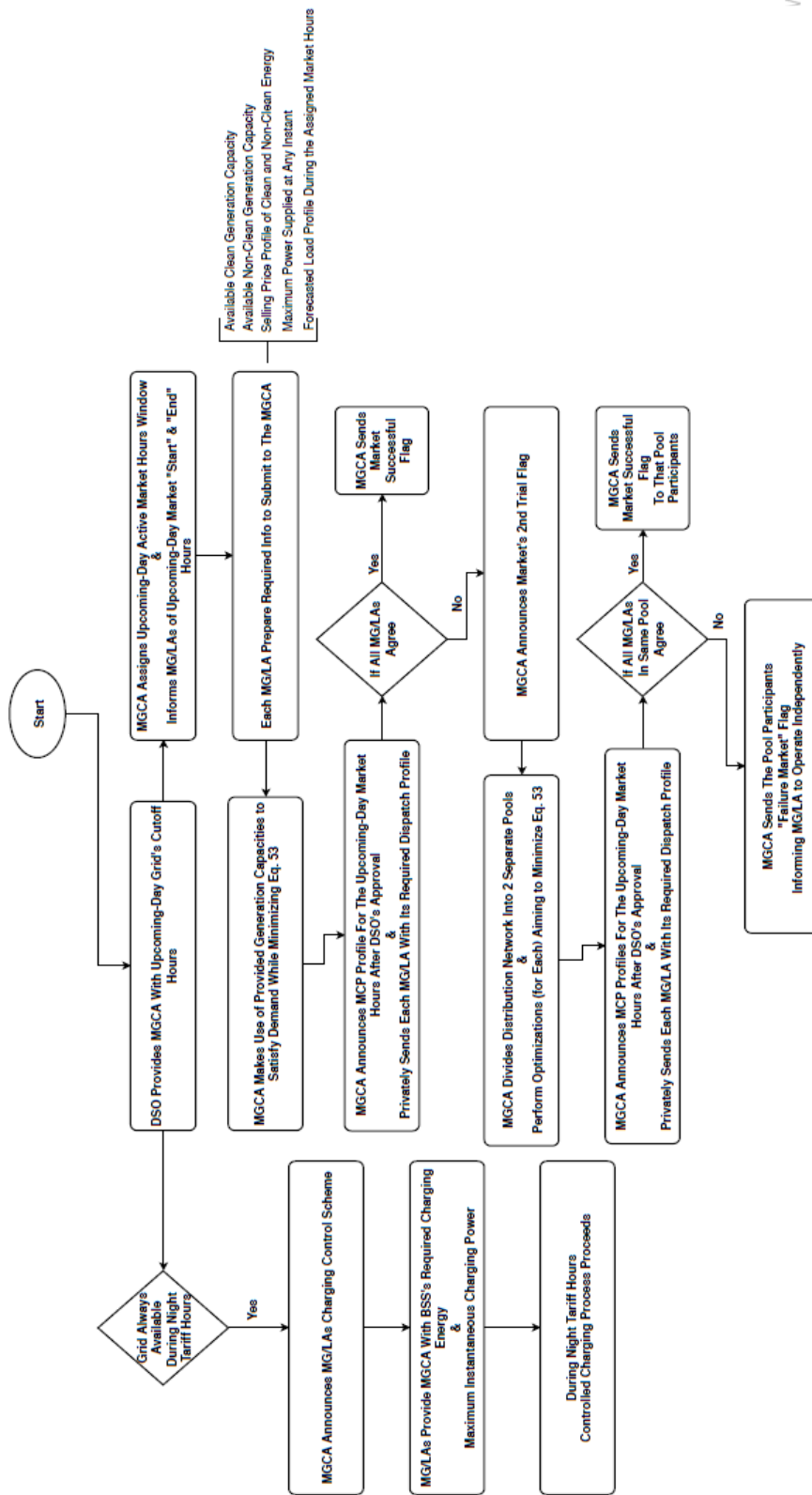
Fig. 8: Cooperation processes

34

d. Computing Market Clearing Price (MCP)

As discussed previously, the proposed market model is pool based, thus none of the participants have the right to sell to/ by from another participant directly except through the MGCA. Furthermore, all energy transactions are priced based on the market clearing price (MCP) calculated by the MGCA.

After receiving each MG/LA bid, generation capacity and demand profile for the upcoming day, MGCA will make use of the provided generation capacities and strike a balance between generation and demand while minimizing distribution network's daily operational cost, diesel dependency and peak hour grid's energy. After configuring the dispatch strategy, MGCA will arrange generating units required to meet the hourly demand and select the operating unit with the highest cost of energy to be the market clearing price. Figure 9 depicts the market clearing price calculation process. The blue curve represents the aggregated generating capacities based on increasing cost of energy, whereas the red curve represents the load demand profile during such hour. The intersection point between the generation and load curve represents the equilibrium point hence the market clearing price.
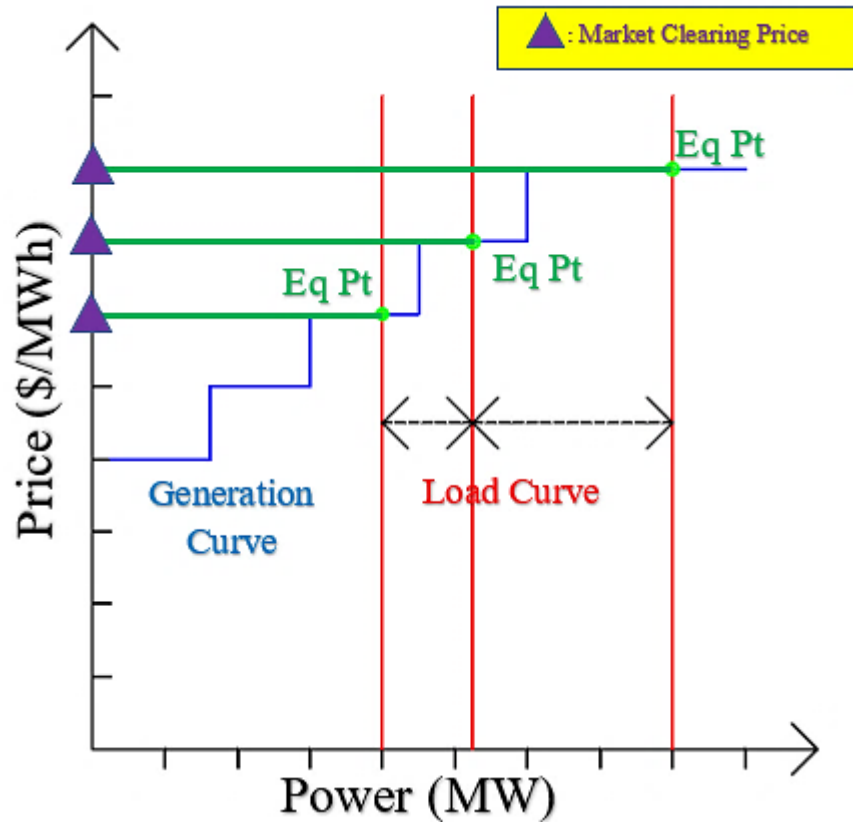
Fig. 9: Supply-demand curves during a certain time "t"

B. 2ⁿᵈ Dimension: Participating Entities

In the case study simulated, different entities were assumed to exist in the distribution network. Each entity has its own characteristics (unique DERs configuration, demand, grid's tariff system), however they all share the same feeder. Thus, all exhibits the same cutoff hours.

1. University Campus

A university campus, subjected to grid's triple tariff rate scheme, is assumed to exist in the distribution network. The campus is assumed to contain 18 buildings. One of these

buildings contain the already existing diesel power plant (marked in red) whereas the rest (marked in blue) are loads.

Initially, the campus is assumed to supply its demand from 2 sources of energy: (1) the unreliable grid and (2) the diesel power plant. The university campus's single line local distribution network diagram and characteristics are shown in figure 10 and table 6 respectively.
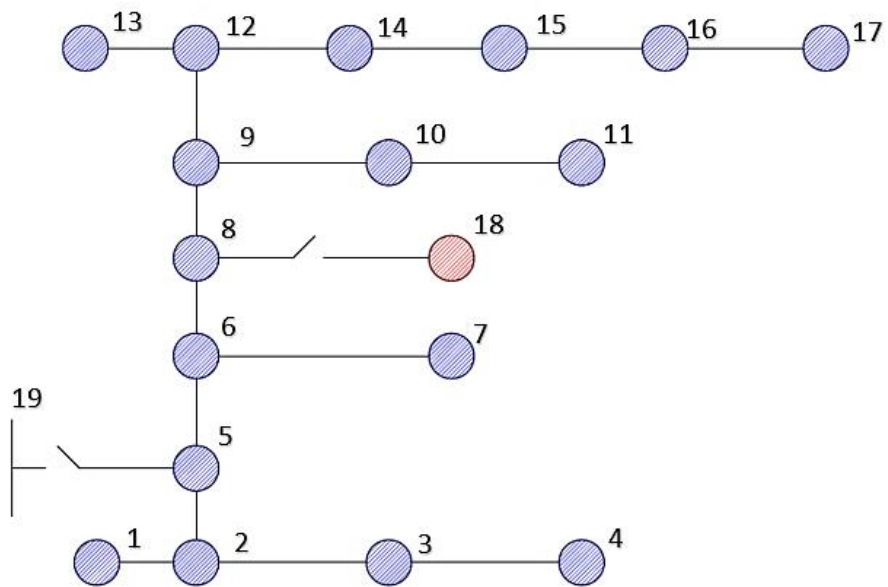
Fig. 10: University campus single line diagram

Table 6: University campus distribution network characteristics

Bus No	Bus No	Length (m)
1	2	91
2	3	76
3	4	99
2	5	198
5	6	76
6	7	99
6	8	76
8	18	152
8	9	61
9	10	61
10	11	91
9	12	76
12	13	46
12	14	76
14	15	76
15	16	76
16	17	152
19 (Grid)	5	114

2. Mall

A mall is the second critical load assumed to exist within the distribution network. Similarly, the mall is assumed to be subjected to the triple tariff scheme illustrated in table 3, and it is assumed to be supplied initially by the unreliable grid and its privately installed diesel power plant. However, unlike the university campus, the mall is assumed to be a large single building (one node).

3. Hospital

The third critical load, consisting of one node and subjected to the triple tariff rate scheme, is assumed to be a hospital. The hospital is also assumed to be initially supplying its demand from unreliable grid's purchased energy and its privately installed diesel generators plant.

4. Residential Microgrids (RMGs)

The distribution network is assumed to contain 3 residential microgrids (RMGs). Each one of them relies on the unreliable grid and a central generation plant consisting of diesel generators and a battery storage system. However, some of the customers within the residential grids are assumed to have a 2kW rooftop PV system installed for private use. The 3 residential microgrids along with each distribution network characteristics are depicted in figure 11 and table 7 respectively. Unlike the previous loads, the residential microgrids are assumed to be subjected to the fixed tariff scheme illustrated in table 3. The assumed generation capacity of each residential microgrid is illustrated in table 8.
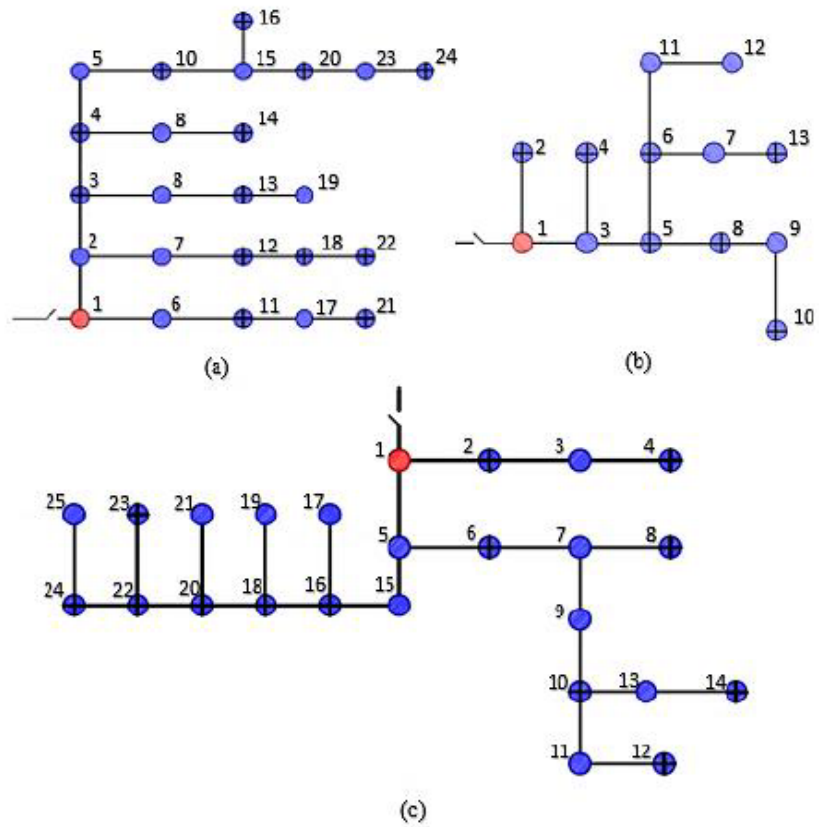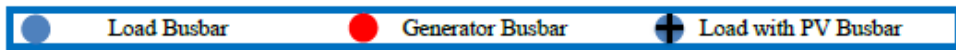
Fig. 11: Residential microgrids' single line diagram

Table 7: Residential microgrids' distribution network characteristics

Residential MG (a)			Residential MG (b)			Residential MG (c)		
Bus No	Bus No	Length (m)	Bus No	Bus No	Length (m)	Bus No	Bus No	Length (m)
1	6	61	1	2	160	1	2	84
6	11	84	1	3	76	2	3	107
11	17	99	3	4	168	3	4	122
17	21	84	3	5	84	1	5	61
1	2	76	5	6	107	5	6	122
2	7	84	6	7	84	6	7	30
7	12	168	5	8	61	7	8	69
12	18	91	8	9	91	7	9	145
18	22	244	0	10	107	9	10	145
2	3	76	6	11	69	10	11	76
3	8	69	11	12	91	11	12	76
8	13	99	7	13	152	10	13	206
13	19	213	1	Grid	91	13	14	145
3	4	84	-	-	-	5	15	213
4	9	69	-	-	-	15	16	137
9	14	175	-	-	-	16	17	53
4	5	99	-	-	-	16	18	84
5	10	137	-	-	-	18	19	69
10	15	91	-	-	-	18	20	69
15	16	175	-	-	-	20	21	91
15	20	38	-	-	-	20	22	69
20	23	160	-	-	-	22	23	84
23	24	99	-	-	-	22	24	91
1	Grid	107	-	-	-	24	25	61
-	-	-	-	-	-	1	Grid	84

Table 8: Residential microgrids' generating capacity

Residential MG (a)		Residential MG (b)		Residential MG (c)	
BSS Capacity	DG Capacity	BSS Capacity	DG Capacity	BSS Capacity	DG Capacity
50kW 125kWh	60kW	35kW 100kWh	38.4kW	50kW 125kWh	70kW

5. *Light Loads*

The distribution network is assumed to also contain 24 different light loads which depend solely on power purchased from the unreliable grid under fixed tariff rate scheme. Thus, suffering from total blackouts during grid's cutoff hours.

Embedding all assumed existing entities, the distribution network is configured as depicted in figure 12.
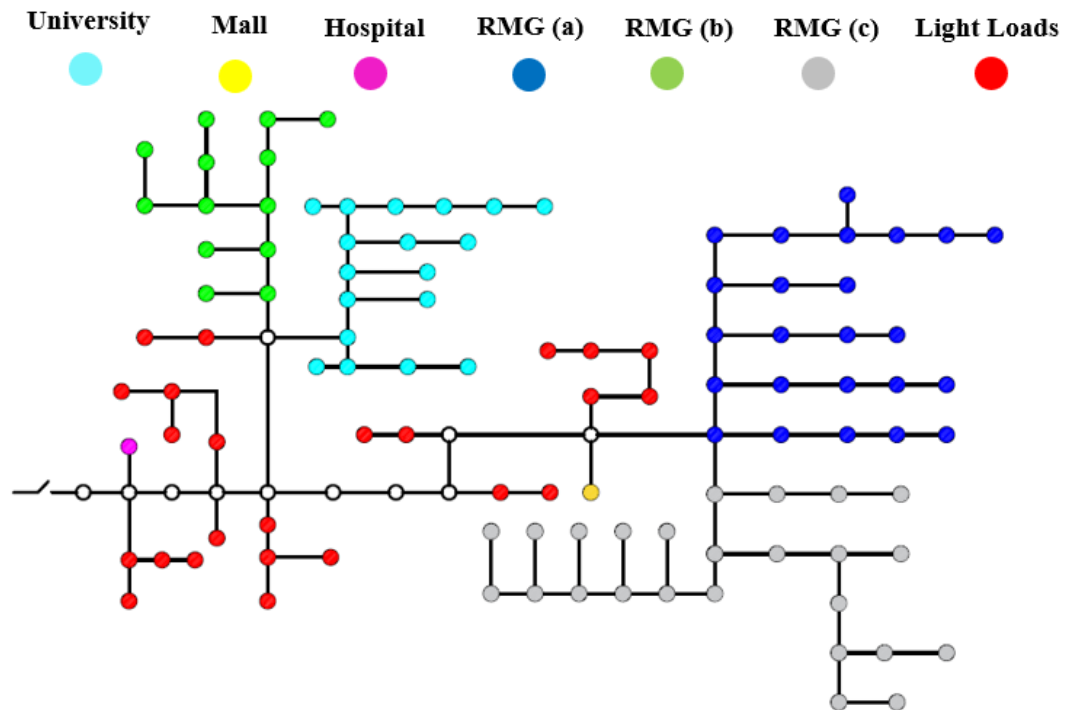
Fig. 12: Reconfigured distribution network

C. 3rd Dimension: Time Sequence

The third dimension governing the proposed market model illustrates the time sequence of the energy trading process. An important feature of the proposed market model is that it doesn't last for the entire next day. It has a certain starting and ending hours that are decided on a daily basis based on the upcoming day's cutoff hour to peak tariff rate hours relation provided by DSO to MGCA. A detailed illustration of how these hours are selected is provided in chapter V.

As depicted from figure 13, the day ahead energy exchange process starts by the MGCA announcing that the gate for each microgrid willing to participate in the upcoming-day-energy-market opens. Submitting bids, forecasted load profiles and generation capacity placed under the MGCA's disposal lasts for a 2-hour period, after which the gate closes. Following that, the MGCA have a 2-hour period to come up with a suitable dispatch strategy (that satisfies his objective) and then provide that strategy to the DSO to check its viability. After the DSO's approval, the MGCA is expected to send each participant its corresponding dispatch profile as well as announcing the cost of energy (MCP) profile during the upcoming day open market hours.

Each participant is provided with a 2-hour period to submit its decision to the MGCA regarding its participation state. If all parties approve, the MGCA sends a successful market sign to all parties, announcing that the energy exchange process starts the next day at an announced hour. However, if the first attempt fails to satisfy all joining parties, the MGCA reconfigures the network into 2 separate pools. The first pool combines critical loads (university, mall, hospital) along with the light loads while the second pool combines residential microgrids together. Then, MGCA repeat his attempt to come up with

a suitable dispatch strategy however under 2 separate market clearing price profiles. Similarly, the MGCA has a 2-hour period to re-send the new dispatch strategies along with the hourly market clearing prices (after the DSO's approval) to each corresponding participant. If all parties within a certain pool approve, MGCA sends the participants of that pool the successful market sign. However, failing to do so, the MGCA send the unsuccessful market sign, informing the pool participants to operate solely during the upcoming day
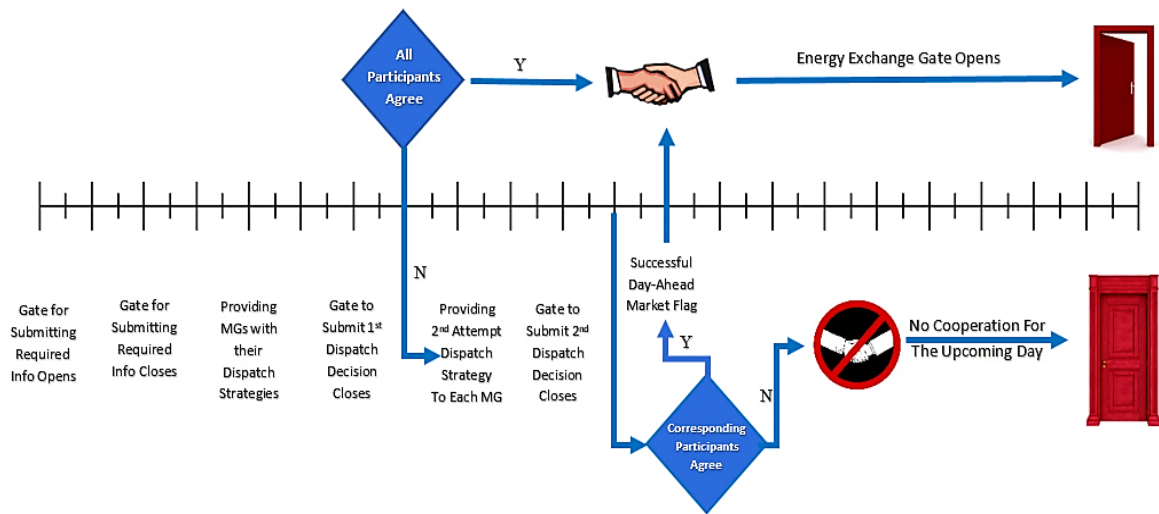
Fig. 13: Energy market exchange process

CHAPTER V

METHODOLOGIES

A. Introduction

The main objective of this study is to test the technical and financial attractiveness of implementing a suitable energy market model combining several participants operating in a distribution network characterized by an unreliable grid and heavy diesel dependency. Thus, in order to clearly test such potential, the problem at hand is divided into 2 main tasks.

The first task is a microgrid level optimization. In this level, the university campus, mall and hospital are assumed to invest in clean energy. Thus, optimizations are performed for each one of them in order to get the optimal configuration (size and site) of a hybrid rooftop-photovoltaic (PV) and battery storage system (BSS) accompanied by an optimal dispatch strategy that satisfies each party's interest. On the other hand, a suitable energy management system is developed for each residential microgrid. The benefits of such optimizations are then provided through comparing the technical and financial merits of the proposed system with the assumed existing one.

The second task is the microgrid community level optimization which represents the platform of the proposed energy market model. In this level, the MGCA is assumed to make use of the provided generation capacities and load profiles to come up with a dispatch

strategy that strikes balance between generation and demand at lowest possible network's daily operational cost while focusing on reducing diesel dependency in first place and grid's peak purchased energy in second place.

Note that market participation decision made by each MG/LA, is based on comparing the daily operational cost attained when following the dispatch provided by the MGCA to that attained under optimal independent operation. Thus, computing the daily operating cost under independent operation for each microgrid is an important task in the proposed market model.

B. Microgrid Level Optimizations

1. University Campus, Mall and Hospital Optimizations

In an attempt to reduce their diesel dependency and grid's peak-hours purchased energy, a PV-BSS investment is proposed. Therefore, the problem at hand is an optimization problem seeking to find the optimal PV-BSS configurations (sizing and siting for university campus, whereas sizing only for mall and hospital) along with deploying an optimal power flow (OPF) energy management system controlling the dispatch of each.

Performing the sizing and siting optimization along with optimal power flow considering the entire yearly data is not a valid approach since it requires a lot of computational time. Thus, a new methodology for sizing and siting was formulated.

The main idea of this methodology is based on characterizing each day by a window of active hours that are determined either by the grid cut-off hour or grid's peak tariff.

Being subjected to a triple tariff scheme, and since the night hours are assigned with low tariffs, such hours are reserved for charging the BSS. Moreover, since the grid is characterized by a daily scheduled 3 hours cutoff period occurring at the times illustrated in table 2, a 4-day period within each month is selected to perform the sizing and siting optimization. Then, after converging to the optimal monthly PV-BSS configurations, the most frequent configuration is selected. Through following such approach, we are able to account for the daily and seasonal variations of the demand, the seasonal climate profile and the daily variations and scheduling of grid blackout hours.

In order to reach the desired objectives, the problem is modelled as a weighted cost minimization function as shown in equation 34.

$$
\min \sum_{day=1}^{4} \left(\sum_{t=h1}^{h2} \left(\gamma P^{grid}(t)\, COE^{grid}(t) + \delta P^{DG}(t)\, COE^{DG} + \varepsilon P^{PV}(t)\, COE^{PV} \right. \right.
$$
$$
\left. \left. + \zeta P^{BSS}_{disch}(t)\, COE^{BSS} \right) + \frac{\gamma \varphi (1 - SOC) \times SOH}{\eta^{BSS}} E_{BSS,rated} \right) \tag{34}
$$

Where, γ, δ, ε, and ζ are the grid, DG, PV and BSS cost weights respectively, φ is the BSS charging cost (\$/kWh) and $E_{BSS,rated}$ is the BSS nominal capacity (kWh).

As illustrated in equation 34, the objective function is divided into 4 periods (4 days), each period is bounded by a unique active hour window starting at h1 and ending at h2. The active hour is denoted by the time intervals during which either the grid is off and DGs are forced to operate or when the purchasing energy from the grid is under peak tariff

rate. During such interval the EMS must decide whether to dispatch the BSS or not. On the other hand, when the grid is ON during other time intervals, (passive hours) grid's tariff is much lower than the BSS cost of energy, hence, discharging them is not an option and so computation time shouldn't be wasted. However, during such hours, an alternative rule-based EMS is deployed to ensure that the demand is supplied by the grid's purchased energy and PV output (if exists) and charges the BSS during night tariff hours.

Equation 34 reveals two weighted cost mechanisms. The first one describes the overall weighted cost during the active hours considered within each day. Whereas the second one corresponds to the weighted cost associated to the charging energy purchased from the grid. The former one helps in converging to a suitable and rational dispatch strategy, whereas the latter acts as a penalty for oversizing the BSS.

The concept of cost weights is due to the fact that the loads under consideration are subjected to a triple tariff (day, night and peak). Thus, the rational approach is to charge the BSS during night tariff (φ) only. Moreover, the EMS aims to minimize diesel dependency and grid's purchased energy during peak tariff hours. Whereas, during day tariff hours and while grid is ON, the demand is supplied from the grid's purchased energy and PV output. Therefore, weights selection is based on the following: (1) there is no penalty on using the PV output power, (2) DGs are the most penalized energy sources, and (3) during day and night tariffs, the demand will be supplied from the PV and grid, whereas BSS will discharge during peak tariff hours after having replaced the DGs during the time when the grid was off.

In order to properly select the weights of the cost function, one must have a high accuracy cost of energy (COE) model suitable to each possible BSS capacity. Unlike the case with PV, BSS is a dispatchable system. Hence, its COE is strongly influenced by its capacity and dispatch strategy. Therefore, in order to have a high accuracy BSS COE model, a rule-based algorithm was deployed on several BSS capacities.

The rule-based algorithm illustrated in figure 14, tries to mimic the desired EMS approach during a whole year period. The built algorithm tries to reduce diesel dependency and grid's peak tariff purchased energy as much as possible while charging the BSS during night tariffs only.
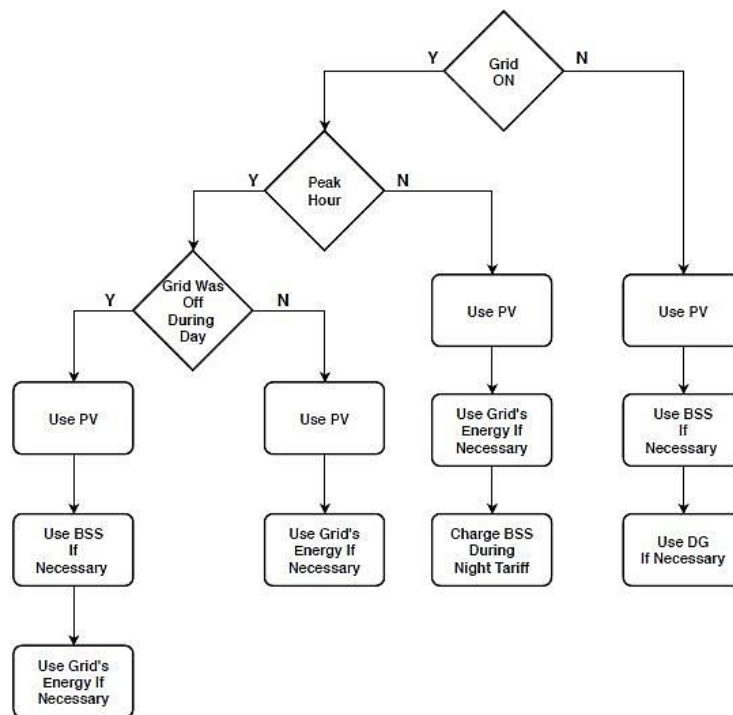
Fig. 14: Rule-based power flow algorithm

49

Then after knowing the annual discharged energy and the annual charging energy for several BSS capacities, the COE for each capacity is computed. Then these values are used to form a BSS COE equation as a function of installed capacity.

Modelling the configuration and the dispatching optimization problem is governed by equations 35 to 52.

$$x^{Univ} = \left[x^{(1)}, x^{(2)}, x^{(3)}, \dots, x^{(18)}, x^{(19)} \right] \tag{35}$$

$$x^{Mall} = \left[x^{(1)}, x^{(2)} \right] \tag{36}$$

$$x^{Hosp} = \left[x^{(1)}, x^{(2)} \right] \tag{37}$$

$$LB^{Univ} = \left[LB^{(1)}, LB^{(2)}, LB^{(3)}, \dots, LB^{(18)}, LB^{(19)} \right] \tag{38}$$

$$UB^{Univ} = \left[UB^{(1)}, UB^{(2)}, UB^{(3)}, \dots, UB^{(18)}, UB^{(19)} \right] \tag{39}$$

$$LB^{Mall/Hosp} = \left[LB^{(1)}, LB^{(2)} \right] \tag{40}$$

$$UB^{Mall/Hosp} = \left[UB^{(1)}, UB^{(2)} \right] \tag{41}$$

$$P_{BSS,rated}^{Univ} = x^{(18)} \tag{42}$$

$$P_{BSS,rated}^{Mall/Hosp} = x^{(2)} \tag{43}$$

$$E_{BSS,rated}^{Univ} = x^{(18)} \times 3 \tag{44}$$

$$E_{BSS,rated}^{Mall/Hosp} = x^{(2)} \times 3 \tag{45}$$

$$0 \leq SOC(t) \leq 1 \tag{46}$$

$$\sum_{t=1}^{t=24} P^{BSS}(t) \leq E_{BSS,rated} \times SOH(t) \times SOC^{prev} \tag{47}$$

$$0 \leq P^{BSS}(t) \leq P_{BSS,rated} \tag{48}$$

$$P^{PV^{(i)}}(t) = x^{(1 \to i)} \frac{P_{PV,AC}(t)}{PV_{rated}^{M}} \tag{49}$$

$$0 \leq P^{DG}(t) \leq P_{DG,rated} \tag{50}$$

$$0 \leq P^{Grid}(t) \leq \infty \tag{51}$$

$$P^{Grid}(t) + P^{DG}(t) + P^{PV}(t) + P^{BSS}(t) = P^{Demand}(t) + P^{Loss}(t) \tag{52}$$

Where, "x" represents the optimization vector holding the configuration details. As mentioned earlier, the university campus contains 18 buildings. Thus, excluding the DG power plant building, the sizing and siting optimization vector is as shown in equation 35. The first 17 indexes represent the installed PV capacity at each building. Whereas the 18th and 19th indexes characterizes the BSS's installed capacity (kW) and its location respectively. On the other hand, the mall and hospital are assumed to be a single node, thus their associated configuration optimization problem is limited to sizing only. Hence, their optimization vector is as shown in equations 36 and 37 where the first index holds the installed PV capacity and the 2nd index describes installed BSS capacity (kW). The lower and upper bound for each optimization vector are selected based on spatial and financial limitations. Note, that in the optimization problem formulated, all values in the optimization vector are assumed to be integer variables.

As observed from equations 44 and 45, the BSS system is designed to provide its rated power for a 3-hour period, where its dispatch strategy is restricted to equations 46, 47 and 48. The instantaneous output power of the installed PV capacity is calculated through multiplying the installed capacity (kW) with the module's expected output to module's rated capacity ratio $\frac{P_{PV,AC}(t)}{PV_{rated}^{M}}$ as shown in equation 49. Equations 50 and 51 illustrates the modelled DG and grid's limits (when grid is ON) respectively. Finally, the last equation used in the optimization modelling is the power balance relation illustrated in equation 52.

2. Residential Microgrids Optimizations

Unlike the scenario assumed with the critical loads (university, mall and hospital), the residential microgrids' configurations are assumed to be known and not optimally selected. Then, the problem at hand deals only with formulating an EMS that benefits each residential microgrid.

The previously proposed EMS will not be suitable in this case, since RMGs are subjected to a fixed grid tariff rate. Hence, a suitable EMS that governs the BSS charging discharging strategy must be formulated. Following a similar concept, RMGs are assumed to operate in a way that reduce diesel dependency without causing excessively higher peaks due to BSS charging. For that case, a suitable rule-based EMS that controls the dispatch of each RMG is proposed.

C. Microgrid Community Level Optimization: Energy Market

All of the previous work done was just to prepare a solid platform for this optimization level. In this level, an energy market is modelled. As previously discussed, the energy market is a combination of several agreements and decisions to be performed by three main participants: (1) the DSO, (2) the MGCA and (3) MG/LAs.

As illustrated in chapter 4, the energy trading process starts by opening the info submission window where MG/LAs submit their generation capacity, their bids and their forecasted load profile for the upcoming day active market window hours. Based on the MGCA's provided information, his objective in this level is to minimize the entire

distribution network's operating cost while stressing on reducing diesel dependency in first place and grid's peak purchased energy in second place. Therefore, the problem is formulated as a weighted cost function shown in equation 53.

$$min \sum_{t=h1}^{t=h2} MCP(t) \times \left(P^{Demand}(t) - P^{PV}(t) \right) + \kappa P^{Grid}(t)\lambda(t) + \xi P^{DG}(t)$$

(53)

$$s.t \quad \lambda = \begin{cases} 1 & \rightarrow during\ peak\ tariff\ hours \\ 0 & Otherwise \end{cases}$$

Where MCP is the market clearing price ($/kWh), κ, ξ are grid's and diesel generator's weights respectively, whereas λ is a binary variable describing grid's peak tariff hours.

Optimization performed by the MGCA is governed by equations 54 to 57.

$$x = \begin{pmatrix} P_1^{BSS^{(t_1)}} & \cdots & P_N^{BSS^{(t_1)}} \\ \vdots & \ddots & \vdots \\ P_1^{BSS^{(t_m)}} & \cdots & P_N^{BSS^{(t_m)}} \end{pmatrix}$$

(54)

$$\sum_{t=1}^{t=m} P_j^{BSS}(t) \leq \sum_{j=1}^{N} E_j^{BSS}$$

(55)

$$P_j^{BSS}(t) \leq P_j^{BSS,Max}$$

(56)

$$P^{Grid}(t) + P^{DG}(t) + \sum_{j=1}^{N} P^{BSS^{(t)}} = P^{Demand}(t) + P^{Loss}(t)$$

(57)

Where, the MGCA is required to find matrix "x" and strike a balance between generation and demand through utilizing the capacities provided by each participant "j" such that the BSS energy used during the market period don't exceed the available capacities as depicted in equation 55 and the instantaneous discharged energy shouldn't violate the maximum permissible limit provided by each participant as shown in equation 56.

D. Algorithms Utilized

1. Genetic Algorithm (GA)

In order to tackle the above-mentioned problems, genetic algorithm (GA) is the first utilized algorithm where it is used to solve the sizing and siting task. GA is heuristic search technique [51] used in computing and in artificial intelligence. Such a technique is an evolutionary one, through which a generation of candidate solutions to an optimization problem is evolved towards better solutions.

The evolution tool is built over three main mechanisms: (1) elitism, (2) crossover, and (3) mutation. At first, the algorithm generates a random feasible population, where such population is then fed to a previously defined fitness function for evaluation. Elitism is performed through ranking individuals within a population based on their performance (fitness value). Where, only elite members (best individuals) are made to survive to the next generation. After selecting the elites of the current generation, a new population is generated consisting of the elite members of the previous one along with new individuals

which are generated through performing the second and third mechanisms (crossover and mutation) on the elites. Thus, a new population is generated having the same number of individuals as the previous one. This described mechanism is made to repeat itself until a stopping criterion is reached [52].

2. Dynamic Programing (DP)

The dispatching problem is a problem governed by a set of sequential decisions. Therefore, dealing with the optimal dispatch problem was conducted through utilizing dynamic programming (DP). DP is a powerful tool used to examine the impacts of decisions taken over a certain horizon. It is frequently used in optimizing microgrid's operation due to its ability to find the optimal feasible dispatch strategy. The algorithm is based on simulating all possible dispatching decision combinations taken during a certain period of time as depicted in figure 15. After building the hourly decision map, the algorithm searches the map for the path achieving the minimum objective function value attained at the end of the horizon.
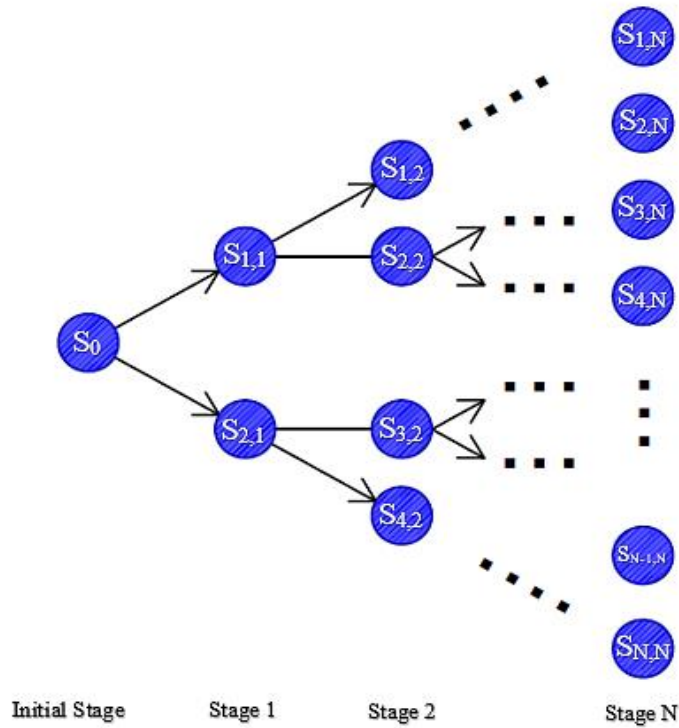
Fig. 15: DP algorithm representation

3. Interior Point Methods (IPM)

IPM is a method that utilizes certain class of algorithms that solve linear and non-linear convex optimization problems. Interior point algorithm tries solving a constrained minimization problem by treating it as a sequence of approximated minimization problems [53]. In the proposed work, IPM was used to solve the problem illustrated by equation 53. IPM was utilized using the "fmincon" function in MATLAB.

4. Gauss-Seidel Numerical Power Flow Analysis Algorithm

As illustrated in equations 52 and 57, power balance is an equality constraint that should be always satisfied. In some studies, where power losses within the distribution network were neglected, power balance constraint was guaranteed through assigning a generation unit with a setpoint equal to the difference between the demand and generation. However, such approach cannot be adopted when accounting for the power losses within the network.

Power losses is a function of the actual nodes' voltage and currents circulating in each link within the distribution network. Hence, involving network's power losses in the equality constraint requires the use of power flow analysis. However, before starting power flow analysis, Y-bus matrix of the network under study must be created. Then, the problem's governing equations can be formulated as follows:

$$Y_{Bus} = \begin{bmatrix} Y_{11} & \cdots & Y_{1n} \\ \vdots & \ddots & \vdots \\ Y_{n1} & \cdots & Y_{nn} \end{bmatrix} \tag{58}$$

$$Y_{ii} = \sum_{j=0}^{n} y_{ij} \tag{59}$$

$$Y_{ij} = -y_{ij} \tag{60}$$

$$\boldsymbol{I_i} = \boldsymbol{V_i} Y_{ii} + \sum_{j=1}^{n} Y_{ij} \boldsymbol{V_j} = \frac{P_i - Q_i}{\boldsymbol{V_{i*}}} \qquad \text{for i} \neq \text{j} \tag{61}$$

As depicted in equation 61, power flow analysis consists of nonlinear equations, then solving such equations requires numerical techniques. Gauss Seidel numerical power

flow solution was adopted, and the equations can be rewritten as shown in equations 62-64, where iterations will be conducted until the difference between power calculated and demand is less than a certain tolerance.

$$V_i^{k+1} = \frac{\frac{P_i - Q_i}{V_i^{*k}} - \sum_{j=1}^{n} Y_{ij} V_j^k}{Y_{ii}} \tag{62}$$

$$P_i^{k+1} = Real\ V_i^{*k} \left[V_i^k Y_{ii} + \sum_{j=1}^{n} Y_{ij} V_j^k \right] \tag{63}$$

$$Q_i^{k+1} = -Img\ V_i^{*k} \left[V_i^k Y_{ii} + \sum_{j=1}^{n} Y_{ij} V_j^k \right] \tag{64}$$

E. Optimization Algorithms Formulated

1. Sizing and Siting Hybrid Algorithm

As mentioned in chapter 5.B.1, the PV-BSS configuration approach was utilized during the active hours (h1 and h2 in equation 34) which are selected based on grid's peak tariff hours or grid's cutoff hours. To be more precise, the active window starts either at the 1st grid's cutoff hour or 1st peak tariff rate hour (whatever comes first) and ends at the last grid's cutoff hour or last grid's peak hour (whatever comes last) during the same day. Whereas, the passive window for that day is the remaining period, where BSS are supposed to charge during night tariff hours.

The flow chart in figure 16 illustrates the exact sizing and siting hybrid approach assigned during the active hours window. As the flow chart reveals, sizing and siting approach was performed through utilizing 3 of the mentioned algorithms: (1) GA, (2) DP, and gauss-seidel based numerical power flow analysis.

The algorithm starts by generating a random feasible (within limits and satisfying constraints) population with a specified number of individuals, where each individual is represented by vector "x". The population generated will be then fed to the GA's fitness function which is illustrated on the right side of figure 16.
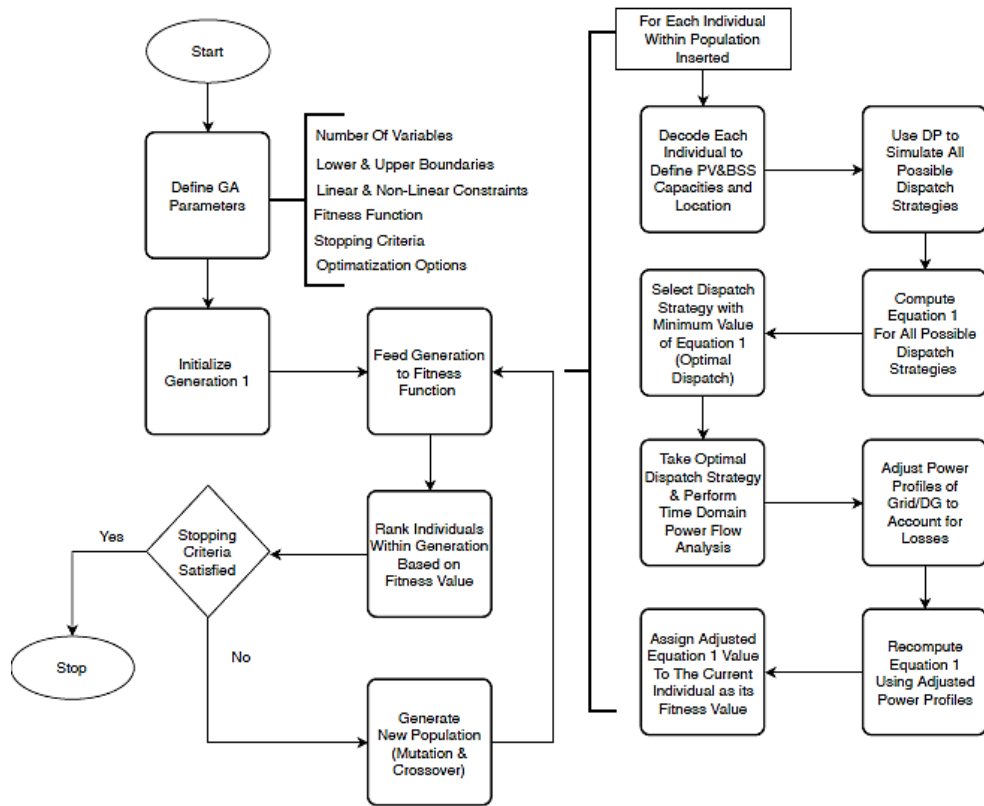

Fig. 16: Sizing and siting hybrid GA-DP-optimal time domain power flow approach

GA's fitness function consists mainly of 2 stages. The first one utilizes DP to simulate all possible dispatch strategies that can be taken during the active hours window. With every passing hour, DP checks between 2 states, the first is "discharge BSS" and the second is "Not to discharge BSS". Since the BSS system is to be charged during night tariff hour which is outside the active hours window, restricting the number of decisions taken by the developed EMS to two states, without including the charging option, is a valid approach that will reduce the search space from 3^t to 2^t, where t corresponds to the hours of continuous simulations.

After running DP, and calculating equation 34 for all possible dispatch combinations, the dispatch strategy that leads to the minimum value of equation 1 is selected as the optimal BSS dispatch strategy to be followed for that individual (PV&BSS configuration).

However, in order to account for the power losses resulted from such PV-BSS configuration operating under optimal dispatch conditions, the optimal BSS dispatch strategy along with the output power of the selected PV capacity is fed to a time domain power flow analysis which represents the 2nd stage in the objective function. In this stage, the optimal dispatch strategy of the BSS along with the instantaneous output PV power of the selected PV capacity are treated as generation setpoints at their assigned locations, and numerical analysis illustrated in equations 58-64 are used to compute the slack unit's (grid or DG during grid's outage) output power. At the end of this period the adjusted grid's and DG's power profile are used to recompute equation 34, and that value is assigned as the individual's fitness value.

After repeating the same process for all individuals within the inserted population, a matrix containing the individuals' characteristics (vector "x") and their associated fitness values is returned to the main GA function for individuals' evaluation. If the best individual fails to satisfy the stopping criteria, the top ranked individuals (elite members) are made to survive to the next generation while the others are discarded, and new generated members occupy their place, preparing for another round of simulations.

2. DP-Rule-Based Optimal Power Flow (OPF) Algorithm

After selecting each MG's (university, mall, hospital) configuration, an annual optimal power flow analysis must be performed in order to observe the microgrid's technical and financial performance. Therefore, making use of the current loads' operating conditions (triple grid's tariff rates) a hybrid DP-Rule-Based optimal power flow algorithm is developed in order to simulate the optimal operation of the reconfigured MGs within a reasonable computational time.

The OPF hybrid algorithm is depicted in figure 17. As depicted from the figure, during each day, expected PV output profile, grid's cutoff schedule, grid's tariff rate profile and the demand profile must be inserted into the EMS. Using the inserted data, the EMS will decides between two modes of operation, (1) running DP to converge for optimal power dispatch strategy or (2) running the rule-based power flow algorithm which is responsible of charging the batteries during night tariffs and supplying the demand via PV power (if exists) and grid's purchased energy.
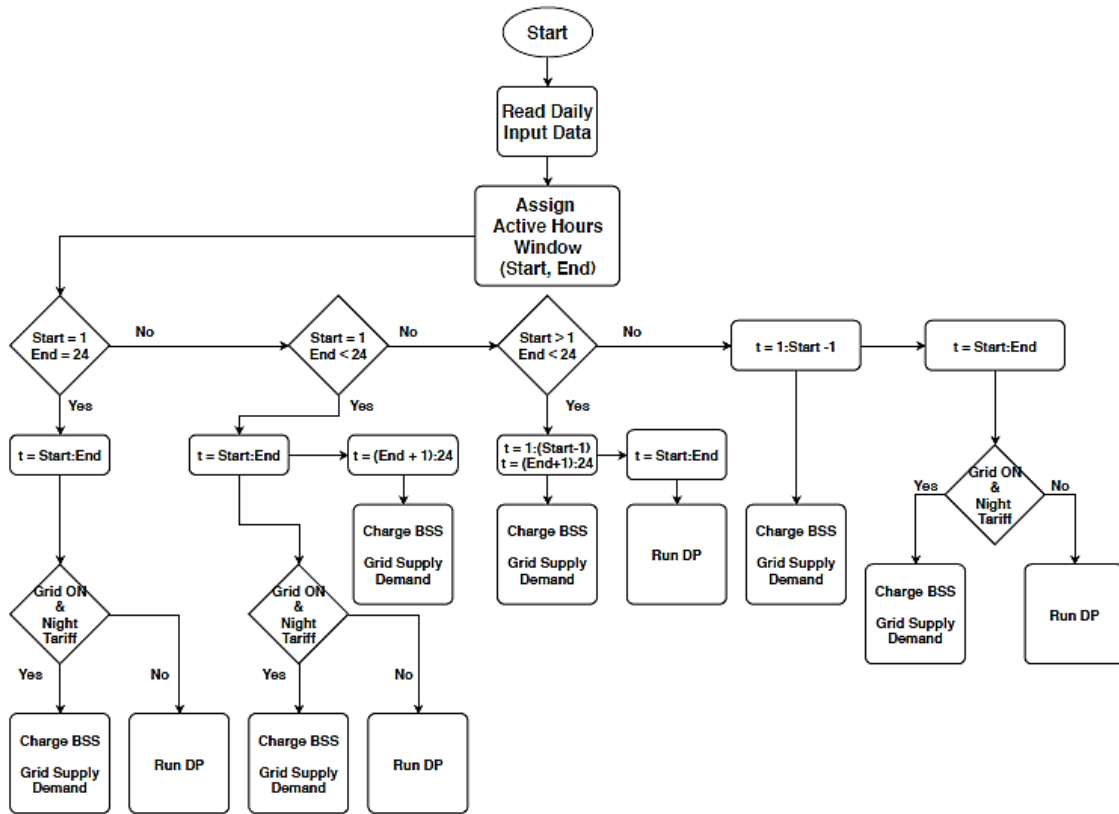
Fig. 17: DP-rule-based optimal annual power flow algorithm

The EMS developed, starts by determining the active hours (Start and End) within the selected day, where during such hours DP mode of operation is selected. Whereas during the remaining day hours, the rule-based approach controlling the charging of the batteries and grid's purchased power is selected. The "Start" hour for the selected day is either the first grid's-outage hour or the first grid's peak hour, whatever comes first. While the "End" is the last grid's-outage hour or the last peak hour, whatever comes last.

Furthermore, if during a certain day, the "Start" hour occurs during the grid's night tariff period, then the EMS system will operate using DP during the period where grid is

Off. Alternatively, when grid is ON again and its tariff is still at its minimum, the EMS will switch to the rule-based approach mode of operation. Rule-based mode of operation will be selected until the grid's next power outage, where DP mode of operation will be conducted again until the last active hour "End" during that day.

Through following such approach and not allowing the DP mode of operation to run during unnecessary operating conditions, the computational time is reduced making it possible to run the EMS for an entire year with an hourly resolution.

Note that in order to account for power losses within the network, at the end of each day's simulation, the BSS optimal dispatch strategy is then fed to the gauss seidel numerical power flow analysis. As previously mentioned, time domain power flow analysis is performed to compute the actual energy extracted from the grid or from the diesel generators (during grid outage) while considering the PV instantaneous output power and BSS dispatch strategy (during discharging) as generation setpoints and considering BSS charging power as an added load to the already forecasted one. Hence, the new adjusted values of the grid's purchased energy and energy extracted from the DGs would account for the power losses within the network.

3. Residential Microgrids' Rule-Based Power Flow Algorithm

Since residential microgrids are subjected to a fixed grid tariff scheme, utilizing the above-mentioned power flow algorithm is not a valid option. Thus, for the case of

residential microgrids, a rule-based power flow algorithm governing the BSS dispatch strategy is proposed.

The proposed algorithm also seeks minimal diesel dependency. However, the BSS charging hours are made to occur in a way that doesn't lead to higher peaks as observed by the grid.
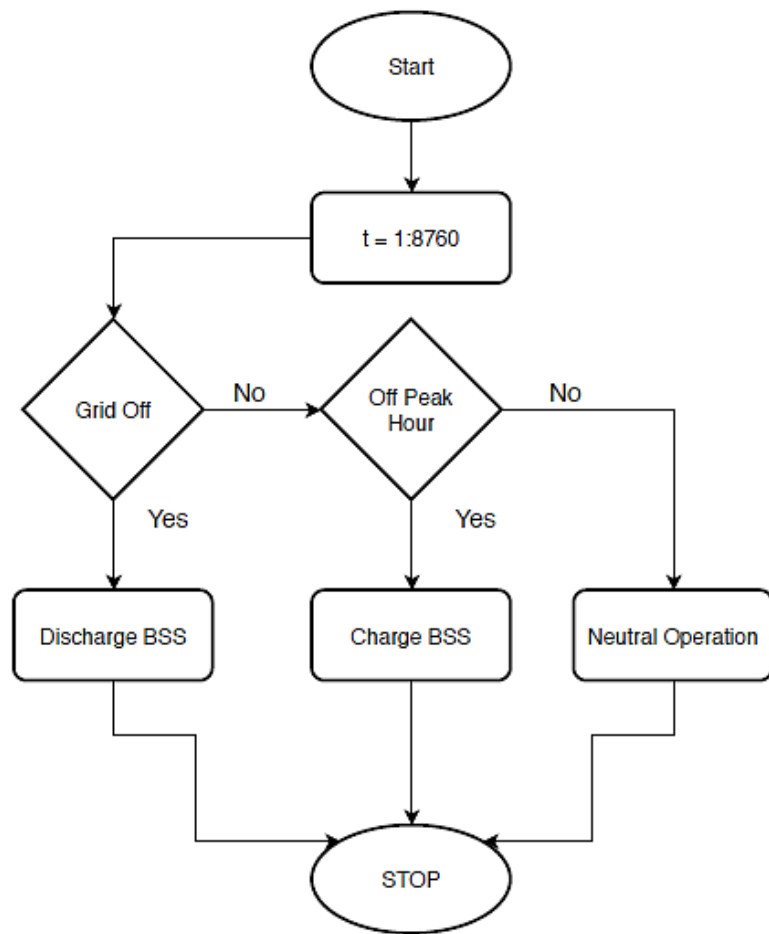
Fig. 18: RMGs' BSS dispatch algorithm

The proposed BSS dispatch algorithm is illustrated in figure 18. During each hour, the EMS tests the grid's state (ON/Off). When the grid is off, the BSS installed capacity must discharge to reduce or completely remove the need of DGs to supply the demand. On the other hand, if grid is on, the EMS controls the BSS charging decision based on the residential microgrid's forecasted load. If peak hour, the EMS decides not to charge the BSS to avoid causing higher peaks to the grid. However, if off-peak hour, the EMS charges the BSS.

4. Market Optimization Algorithm

As illustrated in figure 19, the market optimization utilizes 2 of the mentioned algorithms. IPM is used to converge to the optimal dispatch strategy that minimizes equation 53. However, failing to grab an MG/LA's market participation interest, DP-rule-based power flow analysis, discussed previously, is implemented to guarantee daily optimal operation continuity.

On the other hand, during outside active market window, a rule-based algorithm is utilized to control the BSS's charging process of market participants, if grid was available during entire night tariff period.
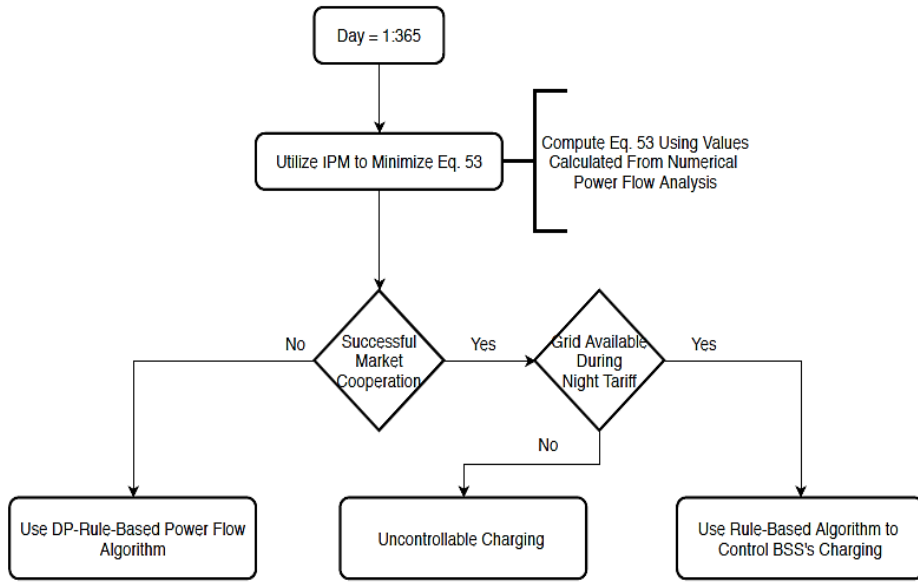
Fig. 19: MGC optimization algorithms

CHAPTER VI

SIMULATION RESULTS

A. Microgrid Optimization Level Results

Table 9: Optimization common input data

ψ	Diesel Cost ($/L)	0.597
γ	Grid's assigned weight 1	3
δ	DG's assigned weight 1	4
ε	PV's assigned weight	1
ζ	BSS's assigned weight	2
κ	Grid's assigned weight 2	4
ξ	DG's assigned weight 2	2
η^{BSS}	BSS's inverter efficiency (%)	95
CC^{PV}	PV's capital cost ($/kW)	874.3
OM^{PV}	PV's O&M cost ($/kW/year)	8.8
CC^{BSS}	BSS's capital cost ($/kW)	1227
OM^{BSS}	BSS's O&M cost ($/kW/year)	4.1
Diesel Generators installed capacity	University Campus (kW)	15,500
	Mall (kW)	14,900
	Hospital (kW)	4,600
	RMG (a) (kW)	60
	RMG (b) (kW)	38.4
	RMG (c) (kW)	70
Diesel Generator's Cost of energy	University Campus (₵/kWh)	26
	Mall (₵/kWh)	25
	Hospital (₵/kWh)	27
	RMG (a) (₵/kWh)	30
	RMG (b) (₵/kWh)	32
	RMG (c) (₵/kWh)	28

The information provided in table 9 summarizes the common input data for each

MG's optimization.

1. *Sizing and Siting Optimization Results*

a. <u>University Campus Microgrid</u>

Table 10: University campus optimization vector's lower and upper bounds

University Optimization Vector	
LB	**UB**
0	285
0	180
0	138
0	65
0	201
0	177
0	100
0	117
0	66
0	95
0	140
0	70
0	180
0	134
0	165
0	136
0	153
6,000	18,000
1	17

Utilizing the PV-BSS configuration approach discussed in section 5.B.1, and restrained by the boundaries summarized in table 10, the optimal monthly PV-BSS configurations are illustrated in table 11.

Table 11: University campus's optimal PV-BSS configurations

Month	Total Optimal PV Cap (kW)	Optimal BSS Cap (kW)	BSS Optimal Location (Busbar #)
January	2,400	9,000	5
February	2,400	9,000	5
March	2,400	8,900	5
April	2,400	9,000	5
May	2,400	9,000	5
June	2,400	9,000	5
July	2,400	10,100	5
August	2,400	9,000	5
September	2,400	9,000	5
October	2,400	9,000	5
November	2,400	9,000	5
December	2,400	9,000	5

Analyzing the results provided in table XI reveals that the optimal PV capacity during all months is 2.4MW, which is the maximum possible installed PV capacity inserted to the optimization problem (sum of PV's upper boundaries). On the other hand, 3 different BSS's capacities were attained: 8.9MW, 9MW being the most frequent and 10.1MW. However, although simulations resulted in 3 distinct optimal BSS capacities, results revealed that busbar 5 in figure 10 is the optimal location of BSS installations. A summary

of the optimal energy share within the active hour window attained for the optimal

configurations illustrated in table 11 is provided in table 12.

Table 12: University's energy share during active window of each optimal PV-BSS
configuration

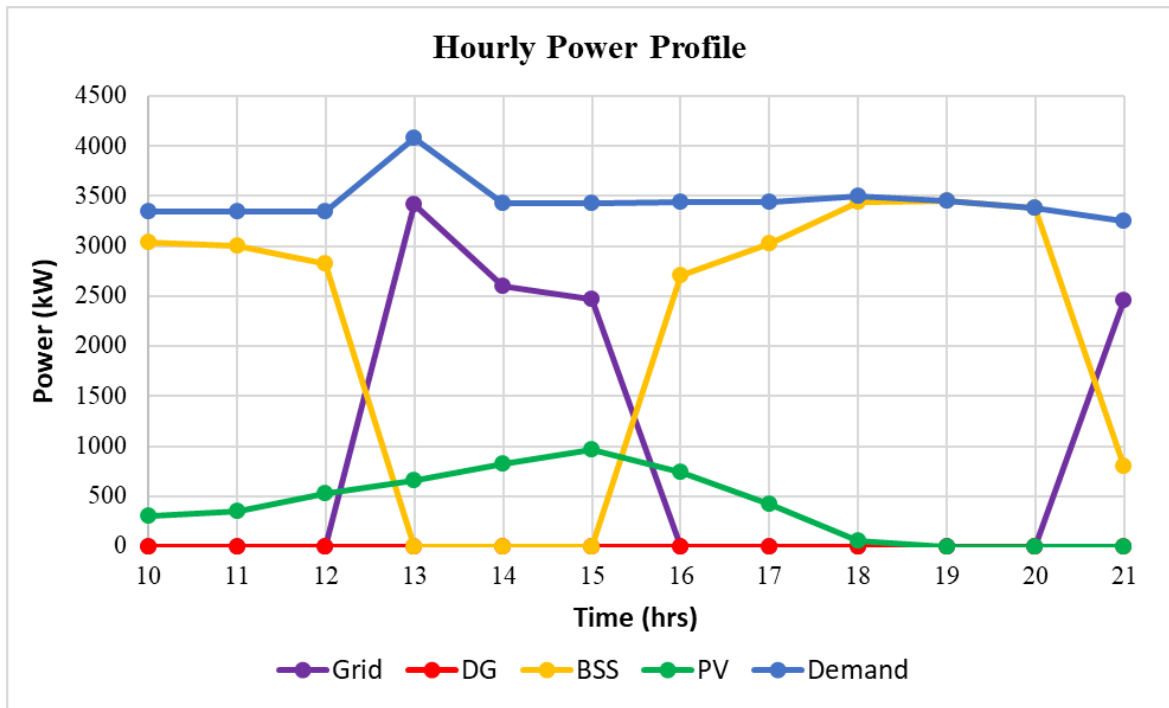| Month	Jan	Feb	Mar	Apr	May	Jun	Jul	Aug	Sep	Oct	Nov	Dec
Grid	50%	56%	51%	50%	49%	60%	69%	67%	70%	67%	64%	57%
DG	0%	0%	0%	0%	0%	0%	0%	0%	0%	0%	0%	0%
PV	10%	12%	15%	17%	19%	16%	10%	11%	10%	10%	9%	9%
BSS	40%	32%	34%	33%	32%	24%	21%	22%	20%	23%	27%	34%

Fig. 20: University campus power flow profile during active hours (10:00 to 21:00) for a
day in January

70

Figure 20 provides a snapshot of the optimal power flow of the university campus with optimal PV-BSS configuration selected during January. Analyzing the figure reveals that no DG energy is used to supply the demand when grid was Off (10:00 pm till 12:00 pm) where the demand is supplied by PV and BSS. In addition, observing the power flow during grid's peak hours (16:00 pm till 21:00 pm), the EMS selects to further discharge the batteries and reduce grid's purchased energy to zero until the last peak hour (21:00 pm).

As observed from table 12, the converged PV-BSS capacities were able to completely remove diesel dependency during the 4-day period of the sizing simulation. However, as suggested previously, the most frequent optimal configuration (2,400kW PV, and 9,000kW BSS) is selected to be the overall optimal configuration for the university campus. Therefore, the optimal PV-BSS technical and financial data for the university campus is as summarized in table 13.

Table 13: University's optimal PV-BSS technical and financial data

Optimal PV Capacity (kW)	2,400
Optimal BSS Capacity (kW – kWh)	9,000 – 27,000
PV Capital Cost ($)	2,098,320
BSS Capital Cost ($)	11,043,000
PV Operational & Maintenance Cost ($/year)	21,120
BSS Operational & Maintenance Cost ($/year)	36,900

b. Mall Microgrid

Table 14: Mall optimization vector's lower and upper boundaries

Mall Optimization Vector	
LB	UB
0	3,200
4,000	16,000

Table 15: Mall's optimal PV-BSS configurations

Month	Optimal PV Cap (kW)	Optimal BSS Cap (kW)
January	3,200	12,800
February	3,200	12,000
March	3,200	12,000
April	3,200	12,000
May	3,200	12,000
June	3,200	11,900
July	3,200	12,700
August	3,200	12,000
September	3,200	12,000
October	3,200	12,000
November	3,200	12,000
December	3,200	12,000

Table 16: Mall's energy share during active window of each optimal PV-BSS configuration

Month	Jan	Feb	Mar	Apr	May	Jun	Jul	Aug	Sep	Oct	Nov	Dec
Grid	52%	51%	50%	46%	46%	45%	45%	49%	45%	44%	48%	48%
DG	0%	0%	0%	0%	0%	0%	0%	0%	0%	0%	0%	0%
PV	9%	12%	12%	18%	19%	21%	20%	17%	18%	16%	12%	11%
BSS	39%	37%	38%	36%	35%	34%	35%	34%	38%	40%	41%	41%

Following similar approach, the monthly optimal PV-BSS configuration and their energy share during the active hours within the 4 simulated days for the mall microgrid, bounded by the values summarized in table 14, are shown in tables 15 and 16.
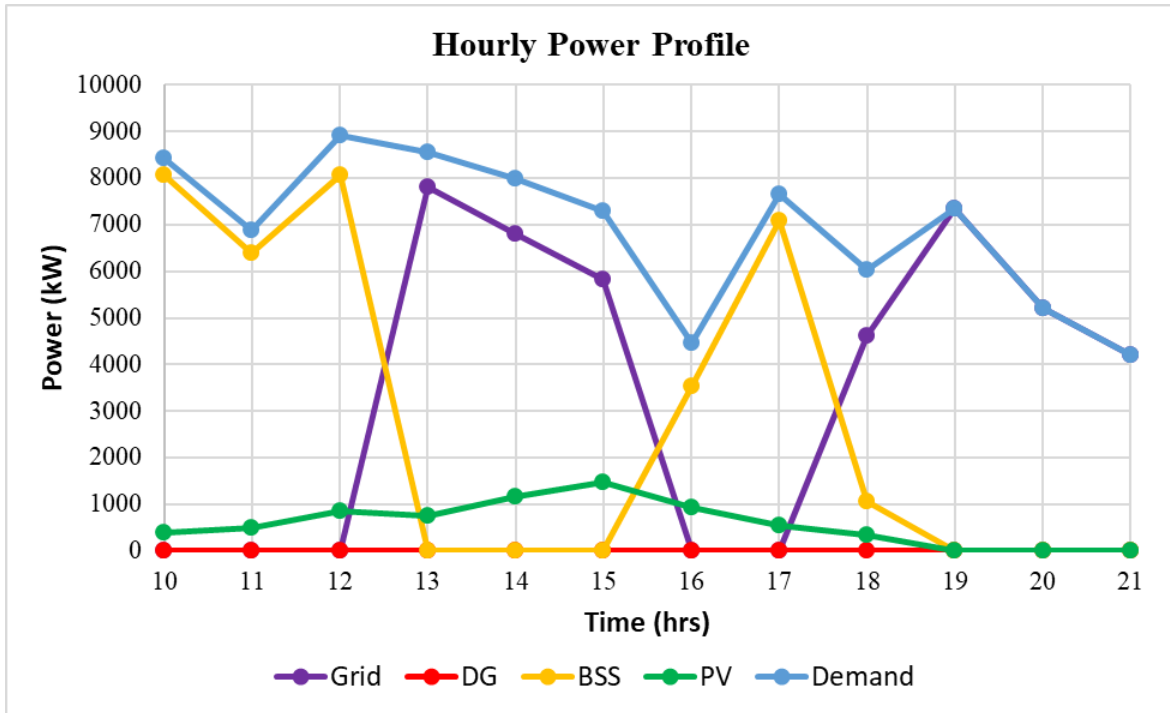
Fig. 21: Mall power flow profile during active hours (10:00 to 21:00) for a day in January

Similarly, analyzing the power dispatch of the optimal PV-BSS configuration attained during January simulations, we observe that the EMS supplied the demand from PV and BSS when the grid was off, and then decided to use the BSS's left energy to replace grid's purchased energy during peak hours.

In this case as well, optimization results revealed that the optimal capacity was the maximum PV system that can be installed within the MG. On the other hand, based on the most frequent optimal BSS capacity attained, a BSS capacity of 12MW-36MWh is selected to be the optimal BSS capacity. Table 17 summarizes the optimal PV-BSS technical and financial characteristics for the mall microgrid.

Table 17: Mall's optimal PV-BSS technical and financial data

Optimal PV Capacity (kW)	3,200
Optimal BSS Capacity (kW – kWh)	12,000 – 36,000
PV Capital Cost ($)	2,797,760
BSS Capital Cost ($)	14,724,000
PV Operational & Maintenance Cost ($/year)	28,160
BSS Operational & Maintenance Cost ($/year)	49,200

c. Hospital Microgrid

The optimization vector in hospital microgrid optimization is bounded as illustrated in table 18. Monthly optimal PV-BSS capacities are provided in table 19.

Table 18: Hospital's optimization vector's lower and upper boundaries

Hospital Optimization Vector	
LB	UB
0	790
700	4,000

Table 19: Hospital's optimal PV-BSS configurations

Month	Optimal PV Cap (kW)	Optimal BSS Cap (kW)
January	790	4,000
February	790	4,000
March	790	4,000
April	790	4,000
May	790	4,000
June	790	4,000
July	790	4,000
August	790	4,000
September	790	4,000
October	790	4,000
November	790	4,000
December	790	4,000

As illustrated in table 19, we observe that both PV and BSS optimal capacities hit the upper limits. Thus, we can conclude that if the hospital was capable of installing larger capacities the algorithm might have converged to bigger configurations.

Checking the optimal dispatch profile for each monthly optimal capacity within the 4 days simulation period, energy share percentages during each period is provided in table 20. As illustrated in table 20, the optimal PV-BSS capacity was capable of almost entirely eliminating diesel's dependency, where only during the first month simulation, 0.1% of demand was supplied by the DGs, whereas diesel was completely eliminated during the other simulation periods. The technical and financial data of the hospital's optimal PV-BSS capacity are provided in table 21.

Table 20: Hospital's energy share during active window of each optimal PV-BSS configuration

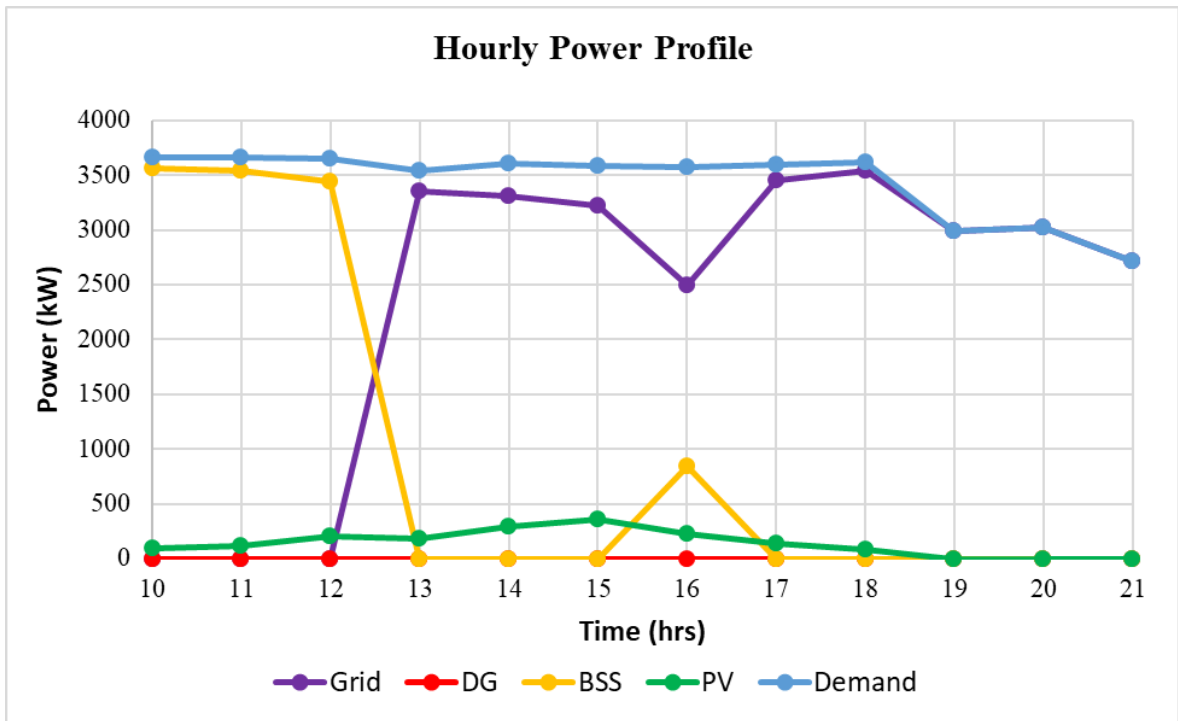| Month	Jan	Feb	Mar	Apr	May	Jun	Jul	Aug	Sep	Oct	Nov	Dec
Grid	75%	70%	72%	71%	67%	64%	66%	68%	69%	70%	74%	72%
DG	0.1%	0%	0%	0%	0%	0%	0%	0%	0%	0%	0%	0%
PV	3.9%	6%	5%	7%	9%	11%	9%	8%	8%	7%	4%	5%
BSS	21%	24%	23%	22%	24%	25%	25%	24%	23%	23%	22%	23%

Fig. 22: Hospital power flow profile during active hours (10:00 to 21:00) for a day in January

Power flow analysis for the optimal PV-BSS configuration during January is provided in figure 22. The power flow depicted in figure 22 provides a strong justification for the

optimization results summarized in table 19. For instance, during the hours between 10:00

am to 12:00 pm, the EMS was using PV & BSS energy to supply the demand. However,

unlike the previous cases (University Campus & Mall), the energy left within the BSS, after

the grid's outage, was only capable of delivering a small fraction of the demand during the

1st peak tariff hour (16:00 pm), then the BSS was completely discharged. Therefore, one

can conclude that any further increase in the possible BSS capacity installed, would

actually lead to a better solution as it causes more decrease in the grid's peak purchased

energy.

Table 21: Hospital's optimal PV-BSS technical and financial data

Optimal PV Capacity (kW)	790
Optimal BSS Capacity (kW – kWh)	4,000 – 12,000
PV Capital Cost ($)	690,697
BSS Capital Cost ($)	4,908,000
PV Operational & Maintenance Cost ($/year)	6,952
BSS Operational & Maintenance Cost ($/year)	16,400

2. Optimal Dispatch Strategies Outcomes

After converging to the university campus, mall and hospital MGs' optimal PV-BSS

configurations, an annual optimal power flow analysis using the algorithms discussed in

5.E.2 and 5.E.3 are conducted in an hourly resolution to test each MG's annual

performance.

a. University Campus Microgrid Annual Performance

Upon comparing the outcomes of the initial and proposed system's annual performance illustrated in table 22, results revealed that the optimal PV-BSS configuration controlled by the dispatch strategy performed by the proposed methodology, decreased DG's dependency to 0.65%, reduced overall system's COE by 27% and scored a net annual saving of $0.578M during the 1st year such system is placed into operation.

Table 22: University campus's initial vs proposed annual performance

	Initial Power System	Proposed Power System
Grid (kWh)	39,978,733	43,534,090
DG (kWh)	6,565,217	370,866
BSS Disch (kWh)	-	9,039,416
BSS Char (kWh)	-	10,009,807
PV (kW)	-	4,014,084
Load (kW)	46,543,950	46,543,950
Total Generation (kWh)	-	56,958,457
Total Demand (kWh)	-	56,553,757
DG Dependency (%)	16%	0.65%
Grid's Cost ($)	3,895,805	3,368,144
DG's Cost ($)	1,706,956	96,425
BSS's Annual Payment ($)	-	1,298,660
PV's Annual Payment ($)	-	260,871
Total Cost ($)	5,602,761	5,024,100
Cost of Energy (₵/kWh)	12	8.9
Savings ($)	578,661	

b. Mall Microgrid Annual Performance

The optimization approach suggested appeared to be a valid one for the mall microgrid as well, as it decreased DG's dependency to 0.22%, reduced overall system's

COE from 13.2₵/kWh to 8.8₵/kWh and resulted in a net annual saving of $0.649M during

the 1st year such system is placed into operation as summarized in table 23.

Table 23: Mall's initial vs proposed annual performance

	Initial Power System	Proposed Power System
Grid (kWh)	33,235,111	36,049,438
DG (kWh)	6,921,291	118,819
BSS Disch (kWh)	-	11,598,909
BSS Char (kWh)	-	12,838,082
PV (kW)	-	5,227,318
Load (kW)	40,156,402	40,156,402
Total Generation (kWh)	-	52,994,484
Total Demand (kWh)	-	52,994,484
DG Dependency (%)	17%	0.22%
Grid's Cost ($)	3,587,444	2,610,643
DG's Cost ($)	1,730,323	29,705
BSS's Annual Payment ($)	-	1,688372
PV's Annual Payment ($)	-	339625
Total Cost ($)	5,317,767	4,668,344
Cost of Energy (₵/kWh)	13.2	8.8
Savings ($)	649,422	

c. Hospital Microgrid Annual Performance

Similarly, although the sizing optimizations for the hospital microgrid suggested

that the optimal PV-BSS configuration was the maximum limits selected, such capacity

was also capable of reducing diesel's dependency to 1% only, while providing a net annual

savings of $0.33M during the first year of placing such system into operation as depicted in

table 24.

Table 24: Hospital's initial vs proposed annual performance

	Initial Power System	Proposed Power System
Grid (kWh)	22,241,527	24,794,316
DG (kWh)	3,735,057	325,691
BSS Disch (kWh)	-	4,059,385
BSS Char (kWh)	-	4,493,302
PV (kW)	-	1,290,494
Load (kW)	25,976,584	25,976,584
Total Generation (kWh)	-	30,469,886
Total Demand (kWh)	-	30,469,886
DG Dependency (%)	13%	1%
Grid's Cost ($)	2,153,454	2,096,856
DG's Cost ($)	1,008,465	87,936
BSS's Annual Payment ($)	-	562,791
PV's Annual Payment ($)	-	83,845
Total Cost ($)	3,161,919	2,831,428
Cost of Energy (₵/kWh)	12.2	9.3
Savings ($)	330,491	

d. Residential Microgrids Annual Performances

Figure 23 illustrates the power flow profile for RMG1 during the 1st day simulation. Analyzing the dispatch shown below, the BSS were discharged between the hours 10:00 am to 12:00 pm during grid's outage. On the other hand, the two spikes observed in grid's energy occurring at 14:00 pm and 16:00 pm refers to the times when the EMS decided to charge the batteries (off peak hours). Therefore, it's clear that the EMS depends on the BSS to supply the demand on first place, whereas DGs are to be used if needed, and charging process is to be done during off-peak hours.
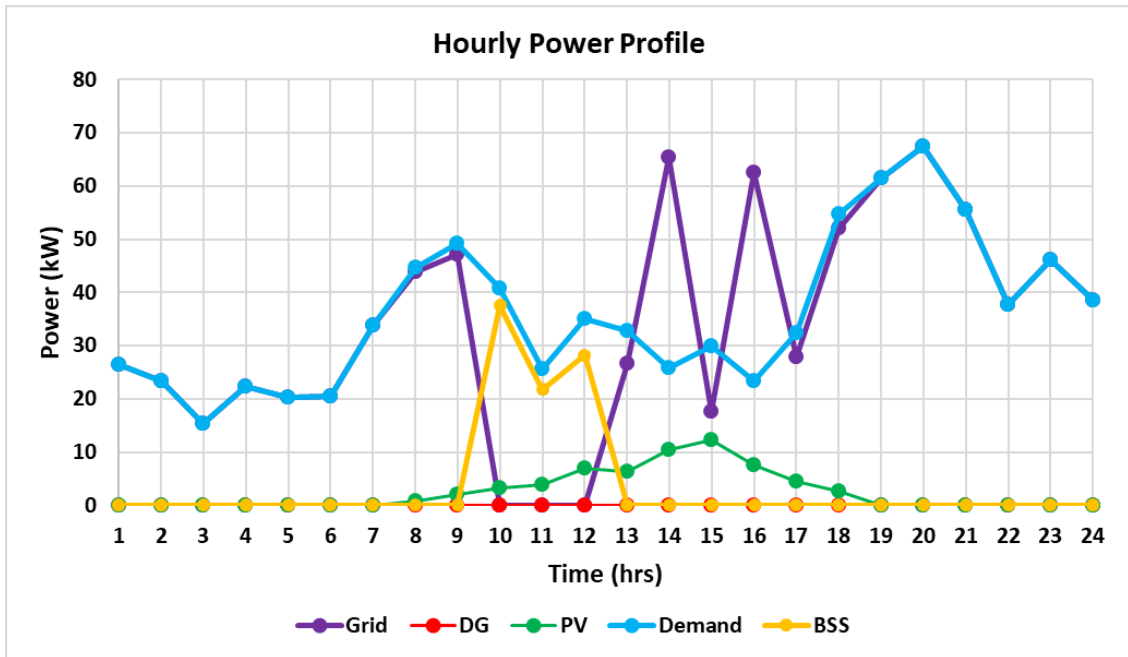
Fig. 23: RMG-1 1st day power flow profile

Table 25: RMG1's technical and financial annual profile

Grid (kWh)	206,720
DG (kWh)	8,300
PV (kWh)	43,528
BSS (kWh)	13,660
Demand (kWh)	257,052
DG Dependency (%)	3.2%
Grid's Cost ($)	27,562
DG's Cost ($)	2490
PV's Annual Payment ($)	3102
BSS's Annual Payment ($)	1191
Total Operating Cost ($)	34,345

Simulating the energy management system discussed in 5.E.3, the annual

performance for the 3 residential microgrids are illustrated in tables 25-27. As noticed,

DG's dependency for the 3 RMGs is minimal, where the maximum annual DG's energy

share didn't exceed 3.2% of the annual energy demand.

Table 26: RMG2's technical and financial annual profile

Grid (kWh)	118,854
DG (kWh)	1,608
PV (kWh)	23,354
BSS (kWh)	10,665
Demand (kWh)	142,658
DG Dependency (%)	1.1%
Grid's Cost ($)	15,847
DG's Cost ($)	515
PV's Annual Payment ($)	1632
BSS's Annual Payment ($)	834
Total Operating Cost ($)	18,828

Table 27: RMG3's technical and financial annual profile

Grid (kWh)	242,525
DG (kWh)	5,105
PV (kWh)	43,429
BSS (kWh)	20,830
Demand (kWh)	289,234
DG Dependency (%)	1.7%
Grid's Cost ($)	32,336
DG's Cost ($)	1,429
PV's Annual Payment ($)	2,962
BSS's Annual Payment ($)	1191
Total Operating Cost ($)	37,919

B. Community Microgrids Optimization Outcomes

Analyzing the difference between the generation and the demand recorded for the university campus and the residential microgrids, we observe that the annual loss energy is insignificant. Therefore, to reduce computational burden, optimizations related to MGC market is performed without accounting for power losses, thus excluding the use of numerical power flow analysis.

The day-ahead market model explained in section 5.E.4 is made to run for an entire year period. Where each microgrid, on a daily basis, has to decide whether to participate in the upcoming day energy market or not. Figure 24 reveals the annual decisions profile made by each of the 6 microgrids. Analyzing figure 24, we observe that the proposed market was considered an attractive alternative for a considerable number of days. Where the it ranges between 235 days (decided by RMG3) and 353 days (decided by hospital MG). Therefore, the market was considered attractive for a minimum percentage of 64% a year.

Recall that, in the hospital sizing optimization problem, all monthly optimal capacities were the upper permissible limits. Thus, we reached to a conclusion stating that the hospital's performance might actually be improved if it has higher capacity limits. The fact that the hospital had the highest market participation decision justifies the previous conclusion, as the required extra capacity is now provided by other participants.
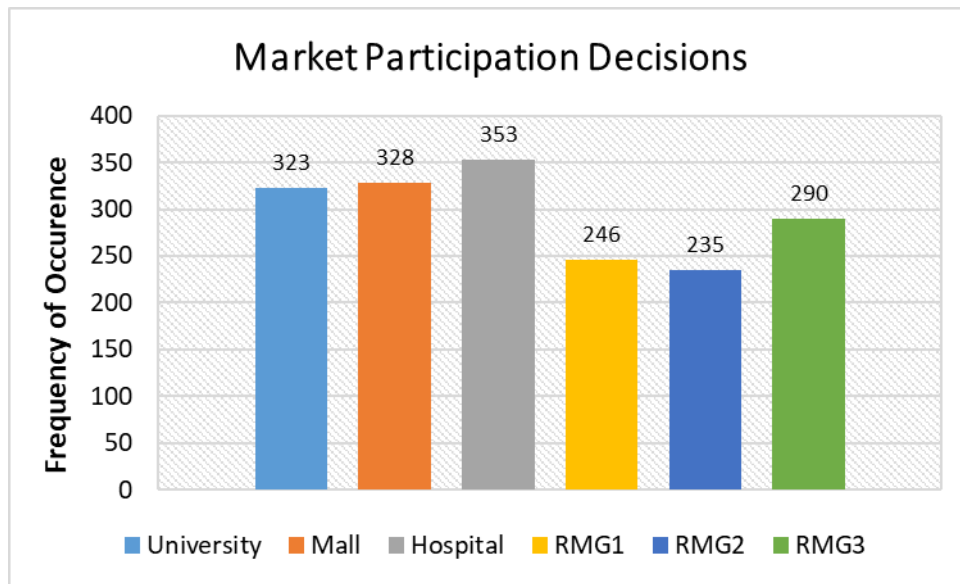
Fig. 24: Annual market participation profile

However, the successful market sign would be announced based on a certain criterion. The successful market is conditioned by either (1) all participant's approval or (2) all participant's approval within a certain pool. As discussed previously, the MGCA will attempt to include all participants in the same pool (phase 1) and if some participants rejected, the process enters phase 2, where 2 separate pools are considered. The first one contains the university campus, mall, hospital microgrids and light loads, while the second combines RMGs together. The bar chart in figure 25, illustrates the frequency of daily market participations received. Figure 25 reveals that during 174 days of the year, the proposed dispatch strategy provided by MGCA was approved by all distribution network participants. On the other hand, 5, 4, 3, 2 and 1 daily market participation decisions were sent to the MGCA 62, 56, 55, 15 and 3 times respectively. The information revealed by figure 25 provides important conclusion. The fact that only 18 days, with daily market

participation frequency less than 3, were recorded, illustrates that participants cooperation is significantly attractive and encouraged.

However, the above information still doesn't provide the exact number of times where the MGCA sends a successful market sign to the MG/LAs. Therefore, to know precisely that number, decisions made by each possible pool is recorded in table 28.
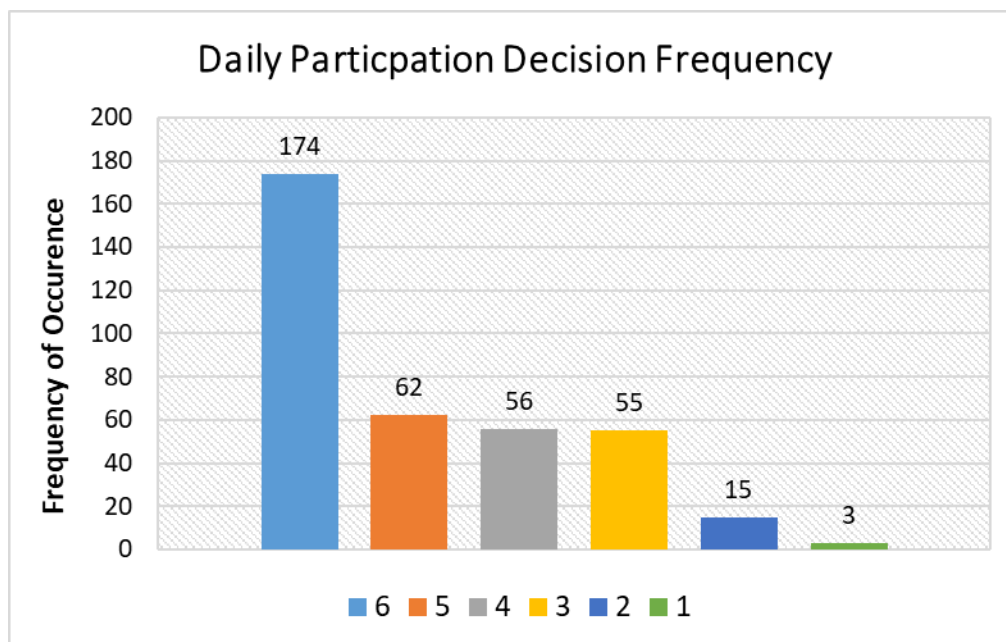

Fig. 25: Daily market participation decision frequency

Table 28: Frequency of successful market sign by pool

Frequency of successful market participations	Pool 1	Pool 2
	285	199

Combining the data provided by figure 25 and table 28, we conclude that the successful

market flag was announced by the MGCA for 310 days within the entire year. A

comparison between independent operation and the proposed market annual performance is

illustrated in table 29.

Table 29: Annual performance of both modes of operation

	Independent Operation Performance	Market Operation Performance
Grid's Energy (kWh)	105,291,762	104,972,274
DG's Energy (kWh)	830,389	863,109
PV's Energy (kWh)	10,642,207	10,642,207
BSS's Energy (kWh)	24,742,865	25,028,861
Demand Energy (kWh)	113,797,744	113,797,744
Demand Shortage (kWh)	86,044	-
University Campus Annual Cost ($)	5,024,100	4,942,794
Mall Annual Cost ($)	4,668,344	4,632,006
Hospital Annual Cost ($)	2,831,428	2,807,332
RMG1 Annual Cost ($)	34,345	33,722
RMG2 Annual Cost ($)	18,828	18,538
RMG3 Annual Cost ($)	37,919	37,382
Total Cost ($)	12,614,964	12,471,774
Savings ($)	143,190	

At a first notice, the proposed market model seems to cause an increase in diesel

generator's dependency as illustrated in table 29. However, the effect is quite the opposite.

Note that for independent operation, light loads were suffering from energy outage, such

energy was supposed to be covered by diesel generators if existed, then taking that into

consideration, the actual diesel energy needed to cover energy demand is 916,433kWh

(DG's energy + shortage). Therefore, comparing that to the one obtained under market operation, we observe that diesel dependency actually decreased by 6%. Similarly, all distribution network participants exhibited a decrease in their annual operational cost causing the entire DN's annual operational cost to be reduced by 143,190$.

A graph showing the market hours window for the 1st day is shown in figure 26, where RMGs' BSS profile is shown to the left of the figure and other participants, including grid, is shown to the right. As discussed previously, the MGCA will make use of the capacities provided by the MG/LA's, along with their respective bids, to satisfy the network's demand and announce the energy spot price profile as illustrated in table 30.
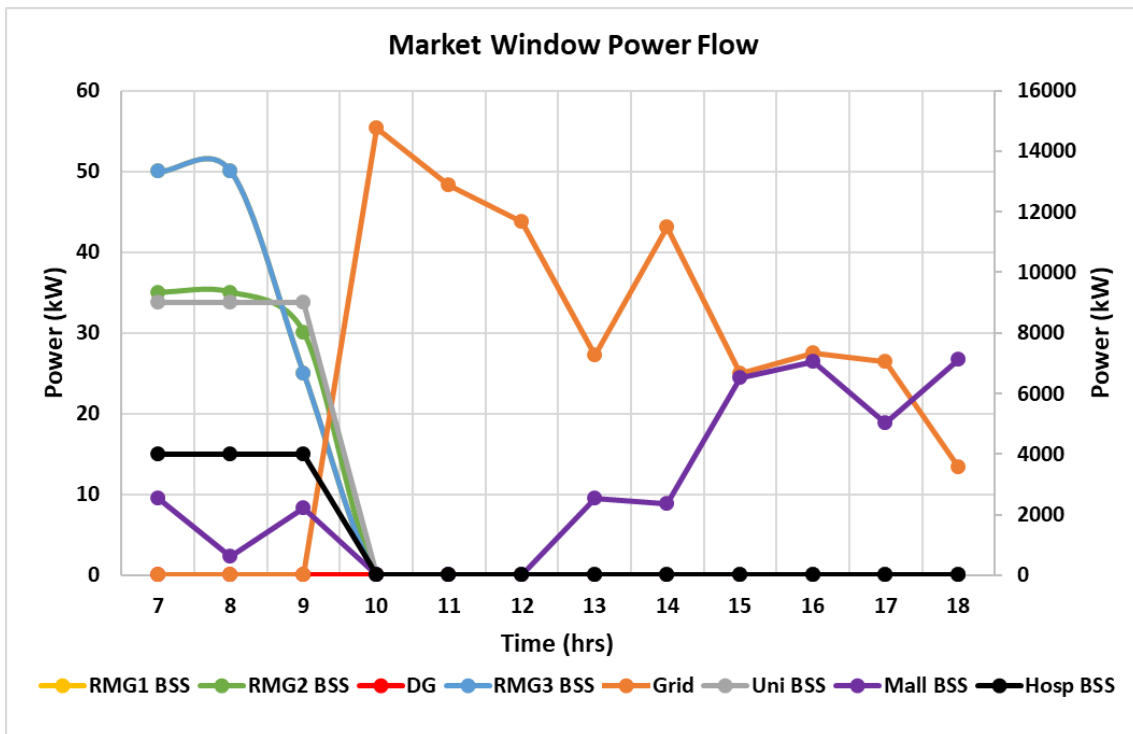

Fig. 26: Power dispatch during 1st day market window

Table 30: Energy prices profile within market hour

Grid	University	Mall	Hospital	RMG1	RMG2	RMG3	MCP
0.000	0.2023	0.2038	0.1969	0.2350	0.2259	0.2049	0.235
0.000	0.2023	0.2038	0.1969	0.2350	0.2259	0.2049	0.235
0.000	0.2023	0.2038	0.1969	0.2350	0.2259	0.2049	0.235
0.075	0.0000	0.0000	0.0000	0.0000	0.0000	0.0000	0.075
0.075	0.0000	0.0000	0.0000	0.0000	0.0000	0.0000	0.075
0.075	0.0000	0.0000	0.0000	0.0000	0.0000	0.0000	0.075
0.213	0.0000	0.2038	0.0000	0.0000	0.0000	0.0000	0.213
0.213	0.0000	0.2038	0.0000	0.0000	0.0000	0.0000	0.213
0.213	0.0000	0.2038	0.0000	0.0000	0.0000	0.0000	0.213
0.213	0.0000	0.2038	0.0000	0.0000	0.0000	0.0000	0.213
0.213	0.0000	0.2038	0.0000	0.0000	0.0000	0.0000	0.213
0.213	0.0000	0.2038	0.0000	0.0000	0.0000	0.0000	0.213

Analyzing table 30, we notice that the MGCA decided to discharge the RMGs' BSS during grid's outage although they provided higher bids, thus causing higher energy market clearing price. Being subjected to fixed grid's tariff scheme, RMG are not allowed to dispatch while grid is ON, and since problem illustrated in equation 53 aims to minimize diesel dependency and grid's peak hour purchased energy, the algorithm converged to a solution were it discharges the RMGs' BSS causing an increase in energy spot market prices during grid's outage and spare that required energy to be discharged during peak tariff hours by other possible participants (mall).

The MGCA, as previously mentioned, provides the DSO with a demand side management task during night tariffs when the grid is always ON. Figure 27 reveals the controlled charging scheme made as to prevent night tariff peaks and smooth the demand, during such hours, as much as possible.
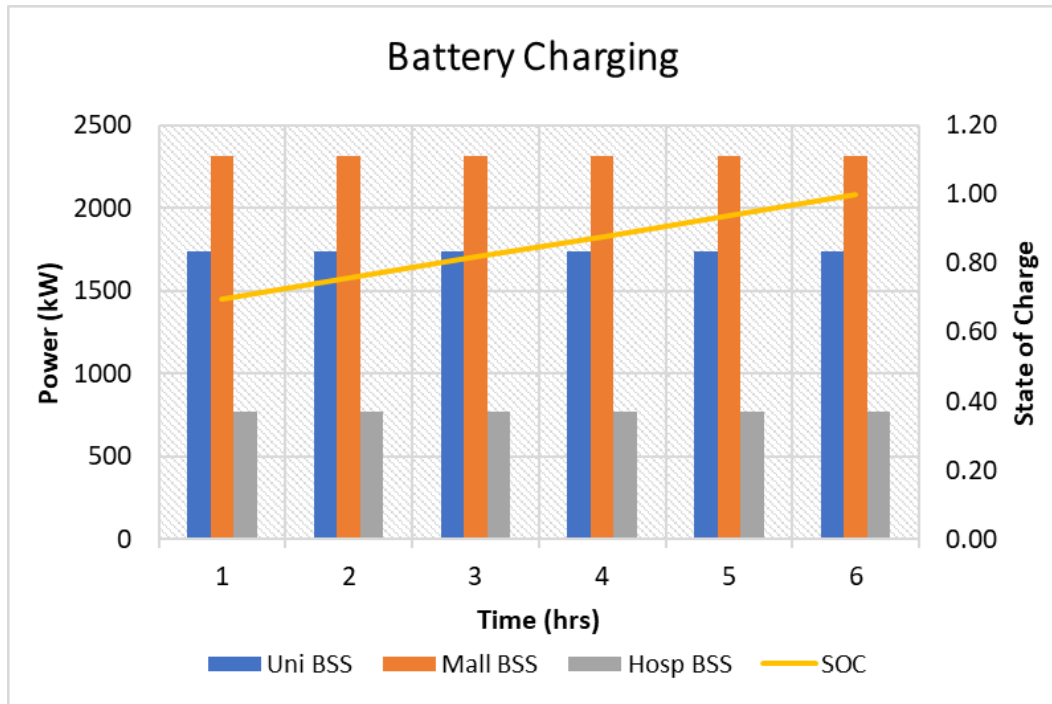
Fig. 27: Controlled night tariff charging

CHAPTER VII

CONCLUSIONS AND FUTURE WORK RECOMMENDATIONS

This work aimed to test the attractiveness of combining distributed energy resources owned by several owners and operating under the influence of an unreliable grid. To test such attractiveness, a two-step optimization process was performed.

The first optimization task dealt with optimizing several major loads with optimal PV-BSS capacities along with an optimal energy management system that minimizes the distribution network's diesel and grid's peak energy dependency. Optimal capacities and dispatch strategies showed significant reduction in the distribution network's participants operational cost, through which annual savings between \$0.33M and \$0.58M were reached for major microgrid while reducing diesel dependency significantly to a maximum of 1% a year.

The second optimization aimed to upgrade the distribution network's performance through creating a suitable market model that governs energy exchange between its participants. The proposed market model was a pool-based day ahead market managed by a microgrid community agent. Whereas, the success of energy trade was based on a daily decision to be taken by the distribution network's participants (microgrid/load agents). The proposed energy market showed further improvements within the distribution network's performance through which it:

1. Covered the energy deficiency of light loads during grid's outage.

2. Reduced annual operational cost by $0.143M.

3. Reduced diesel dependency by 6%.

Improvements achieved in the distribution network's performance, when compared with independent operation, might not be quite large. However, there are still several factors to be included for valid evaluation. For instance, during independent mode of operation spinning reserves' cost was not considered, thus diesel generator's cost was taken to be zero during ON grid times. However, for critical loads, this is not the case, especially that there is a probability of unpredicted grid's outage, and diesel generators are expected to run when battery storage system's state of charge reaches a critical value. Therefore, spinning reserve plays a vital role in correct assessment. Another factor that was not addressed in this study was the cost paid to the distributed system operator for using the grid's distribution network cables and overhead lines as means for exchanged energy. It would also be interesting to check the impact of increasing the available PV capacity on each participant's annual saving. Moreover, for better understanding of proposed market dynamics, a sensitivity analysis can be performed to test the proposed model's outcome in case of diesel fuel cost or grid's tariffs escalations. A further important aspect, accounting for different market policies, can be conducted in order to deploy the best possible market policy for such operating conditions.

In conclusion, although the proposed market model showed slight improvement in the distribution network's operation, further tests and scenarios are still needed for a reliable market evaluation.

BIBLIOGRAPHY

[1]   International Renewable Energy Agency (October 2017). Electricity storage and renewables: costs and markets to 2030. *www.irena.org*.

[2]   Ran, F, Timothy, R, Robert, M. (November 2018). 2018 U.S. Utility-scale photovoltaic-plus-energy storage system costs benchmark. *National Rewable Energy Laboratory*.

[3]   Ali, A., Mohd Nor, N., Ibrahim, T., Fakhizan Romlie, M. (2017). Sizing and placement of battery-coupled distributed photovoltaic generations. *Journal of Renewable and Sustainable Energy* 9 (5): 53501 - 53519.

[4]   Nick, M., Hohmann, M., Cherkaoui, R., Paolone, M. (2013). Optimal location and sizing of distributed storage systems in active distribution networks. *Proceedings of the 2013 IEEE Grenoble Conference,* Grenoble, France (16-20 June 2013).

[5]   Hill, C.A., Such M.C., Chen, D., Gonzalez, J., Grady, W.M. (2012). Battery energy storage for enabling integration of distributed solar power generation. *IEEE Transactions on Smart Grid 3* (2): 850-857.

[6]   Giannitrapani, A., Paoletti, S., Vicino, A., Zarrilli, D. (2017). Optimal allocation of energy storage systems for voltage control in LV distribution networks. *IEEE Transactions on Smart Grid* 8 (6): 2859 – 2870.

[7]   Dasa, C.K., Bassa, O., Kothapallia, G., Mahmoudb, T.S., Habibi, D. (2018). Overview of energy storage systems in distribution networks: placement, sizing, operation, and power quality. *Renewable and Sustainable Energy Reviews* 91 (2018): 1205 – 1230.

[8]   Sok, V., Tayjasanant, T. (2017). Determination of optimal siting and sizing of energy storage system in PV-connected distribution systems considering minimum energy losses. *Proceedings of the 2017 14th International Conference on Electrical Engineering/Electronics, Computer, Telecommunications and Information Technology (ECTI-CON)*, Phuket, Thailand (27-30 June 2017).

[9]   Abou Jawdeh, S.A., Rabih, J. (2012). Mixed integer conic programming approach for optimal capacitor placement in radial distribution networks. *Proceedings of the 47th International Universities Power Engineering Conference (UPEC)*, London, UK (4-7 September 2012).

[10] Rabih, J. (2006). Radial distribution load flow using conic programming. *IEEE Transactions on Power Systems* 21 (3):1458 – 1459.

[11] Rabih, J., Ravindra, S., Bikash, P. (2012). Minimum loss network reconfiguration using mixed-integer convex programming. *IEEE Transactions on Power Systems* 27 (2):1106 – 1115.

[12] Rabih, J. (2012). Solution to economic dispatching with disjoint feasible regions via semidefinite programming. *IEEE Transactions on Power Systems* 27 (1):572 – 573.

[13] Rabih, J. (2012). Optimization of AC transmission system planning. *IEEE Transactions on Power Systems* 28 (3):2779 – 2787.

[14] Steven, L. (2014). Convex relaxation of optimal power flow-part 1: formulations and equivalence. *IEEE Transactions on Control of Network Systems* 1 (1):15 – 27.

[15] Mostafa, N., Rachid, C., Mario, P. (2014). Optimal allocation of dispersed energy systems in active distribution networks for energy balance and grid support. *IEEE Transactions on Power Systems* 9 (5): 2300 – 2310.

[16] Joshua, T., Franz, H. (2012). Convex models of distribution system reconfiguration. *IEEE Transactions on Power Systems* 27 (3): 1407 – 1413.

[17] Liao, J.T., Chuang, Y.S., Yang, H.T., Tsai, M.S. (2018). BESS-Sizing optimization for solar PV system integration in distribution grid. *IFAC PapersOnLine* 51 (28): 85 – 90.

[18] Raptis, D.A., Periandros, P.S., Gkaidatzis, P.A., Bouhouras, A.S., Labridis, D.P. (2018). Optimal siting of BESS in distribution networks under high PV penetration. *Proceedings of the 2018 53rd International Universities Power Engineering Conference (UPEC),* Glasgow, UK (4-7 September 2018).

[19] Sandhu, K.S., Mahesh, A. (2016). A new approach of sizing battery energy storage system for smoothing the power fluctuations of a PV/wind hybrid system. *International Journal of Energy Research* 40 (9): 1221 – 1234.

[20] Md Alamgir, H., Hemanshu, P., Stefano, S., Forhad, Z., Kashem, M. (2019). Energy management of community microgrids considering degradation cost of battery. *Journal of Energy Storage* 22 (2019):257 – 269.

[21] Babacan, O., Torre, W., Kleissl, J. (2017). Siting and sizing of distributed energy storage to mitigate voltage impact by solar PV in distribution systems. *Solar Energy* 146 (2017): 199 – 208.

[22] Arabali, A., Ghofrani, M., Etezadi-Amoli, M., Fadali, M.S., Baghzouz, Y. (2013). Genetic-Algorithm-Based optimization approach for energy management. *IEEE Transactions On Power Delivery* 28 (1): 162 – 170.

[23] Babacan, O., Torre, W., Kleissl, J. (2016). Allocation of battery energy storage systems in distribution networks considering high PV penetration. Master thesis. University of California, San Diego.

[24] Salee, S., Wirasanti, P. (2018). Optimal siting and sizing of battery energy storage systems for grid-supporting in electrical distribution network. *Proceedings of the 2018 International ECTI Northern Section Conference on Electrical, Electronics, Computer and Telecommunications Engineering (ECTI-NCON),* Chiang Rai, Thailand (25-28 Feb. 2018).

[25] Mansuwan, K., Jirapong, P., Burana, S., Thararak, P. (2018). Optimal planning and operation of battery energy storage systems in smart grids using improved genetic algorithm based intelligent optimization tool. *Proceedings of the 2018 International Conference and Utility Exhibition on Green Energy for Sustainable Development (ICUE)*, Phuket, Thailand (24-26 Oct. 2018).

[26] Pires, V.F., Lopes, R., Costa, D. (2018). Integration of storage systems in distribution networks through multiobjective optimization. *Electrical Engineering* 100 (3): 1939 – 1948.

[27] Jahangir, H., Ahmadian, A., Golkar, M.A. (2015). Multi-Objective sizing of grid-connected micro-grid using pareto front solutions. . *Proceedings of the 2015 IEEE Innovative Smart Grid Technologies - Asia (ISGT ASIA),* Bangkok, Thailand (3-6 Nov. 2015).

[28] Alramlawi, M., Gabash, A. (2017). Optimal operation strategy of a hybrid PV-battery system under grid scheduled blackouts. *Proceedings of the 2017 IEEE International Conference on Environment and Electrical Engineering and 2017 IEEE Industrial and Commercial Power Systems Europe (EEEIC / I&CPS Europe)*, Milan, Italy (6-9 June 2017).

[29] Amrit, P., Kalpesh, C., Chao, L., Hoay, G. (2019). Peer-to-peer energy trading in a prosumer-based community microgrid: a game-theoretic model. *IEEE Transactions on Industrial Electronics* 66 (8):6089 – 6097.

[30] Chenghua, Z., Jianzhong, W., Yue, Z., Meng, C., Chao, L. (2018). Peer-to-peer energy trading in a microgrid. *Applied Energy* 220 (2018):1 – 12.

[31] Ahmed, B., Bhaskar, R., Martin, M. (2015). Open energy market strategies in microgrids: a stackelberb game approach based on a hybrid multiobjective evolutionary algorithm. *IEEE Transactions on Smart Grid* 6 (3):1243 – 1251.

[32] Long, C., Wu, J., Zhou, Y., Jenkins, N. (2018). Aggregated battery control for peer-to-peer energy sharing in a community Microgrid with PV battery systems. *Energy Procedia* 145 (2018): 522-527.

[33] Long, C., Wu, J., Zhou, Y., Jenkins, N. (2018). Peer-to-peer ennergy sharing through a two-stage aggregated battery control in a community microgrid. *Applied Energy* 226 (2018):261 – 276.

[34] Pourya, S., Huaiqi, X., Ayomide, L., Jhi-Young, J. (2016). Economic dispatch for an agent-based community microgrid. *IEEE Transastions on Smart Grid* 7 (5): 2317 – 2324.

[35] Nand, M., Jin, Y., Evan, Z. (2019). Optimal planning and operational management of open-market community microgrids. *Energy Proceedia* 159 (2019): 533 – 538.

[36] Hayes, B.P., Thakur, S., Breslin, J.G. (2020). Co-simulation of electricity distribution networks and peer to peer energy trading platforms. *Electrical Power and Energy Systems* 115 (2020):105419.

[37] Zhiyi, L., Shay, B., Alek, P., Mingya, Y., Mohammad, S. (2019). Blockchain for decentralized transactive energy management system in networked microgrids. *The Electricity Journal* 32 (4): 58 – 72.

[38] Wessam, B., Peter, T., Ulrich, W. (2019). Integration of energy markets in microgrids: a double-sided auction with device-oriented bidding strategies. *Applied Energy* 241 (2019): 625 – 639.

[39] Nguyen, S., Wei. P., Peter, S., Damminda, A., Xinghou, Y. (2018). Optimizing rooftop photovoltaic distributed generation with battery storage for peer-to-peer energy trading. *Applied Energy* 228 (2018): 2567 – 2580.

[40] Zhang, Z., Wang, H., Qin, Y., GU, C., Chen, D., Yin, K. (2019). A optimization strategy of a microgrid energy market based on scenario method. *Proceedings of 3rd Information Techonology, Networking, Electronic and Automation Control (ITNEC)*, Chengdu, China (15-17 March).

[41] Tian, P., Xiao, X., Wang, K., Ding, R. (2016). A hierarchical energy management system based on hierarchical optimization for microgrid community economic operation. *IEEE Transactions on Smart Grid* 7 (5): 2230- 2241.

[42] Ismail, M.S., Moghavvemi, M., Mahlia,T.M.I. (2013). Techno-economic analysis of an optimized photovoltaic and diesel generator hybrid power system for remote houses in a tropical climate. *Energy Conversion and Management* 69 (May 2013): 163-173.

[43] Lopez, R., Agustin, J., Loyo, J., Navarro, J., Rosado, I., Rosado, R., Lujano, J., Aso, I. (2011). Multi-objective optimization minimizing cost and life cycle emissions of stand-alone PV–wind–diesel systems with batteries storage. *Applied Energy* 88 (11): 4033-4041.

[44] Mohamed, M.A., Eltamaly, A.M., Alolah, A.I. (2015). Sizing and techno-economic analysis of stand-alone hybrid photovoltaic/wind/diesel/battery power generation systems. *Journal of Renewable and Sustainable Energy* 7 (063128): 1-18.

[45] Koutroulis, E., Kolokotsa, D., Potirakis, A., Kalaitzakis, K. (2006). Methodology for optimal sizing of stand-alone photovoltaic/wind-generator systems using genetic algorithms. *Solar Energy* 80 (9): 1072-1088.

[46] Van Sark, G J H M W. (2007). Teaching the relation between solar cell efficiency and annual energy yield. *European Journal of Physics* 28 (3): 415-427.

[47] Singh, R., Sharma, M., Rawat, R., Banerjee, C. (2018). An assessment of series resistance estimation techniques for different silicon based SPV modules. *Renewable and Sustainable Energy Reviews* 98 (December 2018): 199-216.

[48] Yang, J., Sun, Y., Xu, Y. (2013). Modeling impact of environmental factors on photovoltaic array performance. *International Journal of Energy and Environment* 4 (6): 955–968.

[49] LG (2009). LG LG365Q1C-A5. https://www.lg.com/us/business/solar-panel/all-products/lg-LG365Q1C-A5. Accessed March 6, 2019.

[50] Gunawardana, A.G. (2014). Proper sizing of energy storage for grid connected photovoltaic system. Master thesis. University of Agder.

[51] Techopedia (2019). Genetic algorithm. https://www.techopedia.com/definition/17137/genetic-algorithm. Accessed March 6, 2019.

[52] Konak A, Coit DW, Smith AE. (2006). Multi-objective optimization using genetic algorithms: a tutorial. *Reliab Eng Syst Safe* 91(9): 992-1007.

[53] Wikipedia (2020). Interior-point method. https://en.wikipedia.org/wiki/Interior-point_method. Accessed February 8, 2020.